PEOPLE'S DEMOCRATIC REPUBLIC OF ALGERIA

Ministry of Higher Education and Scientific Research

University of Amar Telidji - Laghouat

Faculty of Technology

Department of Electronics

MASTER THESIS

DOMAIN: Science & Technology

FIELD: Automation

SPECIALTY: Automation & Industrial Computing

MENNAD MERIEM

Theme

Tracking of the GMPP for a Photovoltaic generator using Model- Free Control and Particle Swarm Optimisation

Jury members:

HADJAISAA Aboubakeur	MCA	President
BOUGRINE Mohammed djamel	MCB	Examiner
ABOUCHABANA Nabil	MCB	Supervisor
AMEUR Khaled	MCB	Co-Supervisor

2023 / 2024

Abstract

This project investigates advanced Maximum Power Point This thesis investigates advanced MPPT techniques and control strategies for enhancing PV system performance under partial shading conditions. It compares Perturb and Observe (P&O) with Particle Swarm Optimization (PSO), integrating Proportional-Integral (PI) controllers and Model-Free Control (MFC). Through simulations, the study assesses the accuracy and stability of these methods.

Résumé

Ce projet examine les techniques avancées de suivi du Point de Puissance Maximale Global (GMPPT) et les stratégies de contrôle pour améliorer les performances des systèmes photovoltaïques sous conditions de ombrage partiel. Il compare les techniques Perturb and Observe (P&O) avec l'optimisation par essaim de particules (PSO), intégrant des régulateurs proportionnels-intégrateurs (PI) et le contrôle sans modèle (MFC). À travers des simulations, l'étude évalue la précision et la stabilité de ces méthodes.

ملخص: تبحث هذه الأطروحة في تقنيات التتبع المتقدم لنقطة القدرة القصوى (MPPT) واستراتيجيات التحكم لتحسين أداء نظام الطاقة الشمسية تحت ظروف التظليل الجزئي. وتقارن بين طريقة التذبذب والملاحظة (P&O) وطريقة تحسين سرب الجسيمات (PSO)، مع دمج وحدات التحكم التناسبية التكاملية (PI) والتحكم الخالي من النماذج (MFC). ومن خلال المحاكاة، تقيم الدراسة دقة واستقرار هذه الأساليب.

Acknowledgements

I would like to express my special appreciation and thanks to my supervisors Mr. ABOUCHABANA Nabil and Mr. AMEUR Khaled. I would like to thank them for encouraging my research and for facilitating the way to accomplish my master thesis. I would also like to thank the committee members,Dr. HADJAISAA Aboubakeur, Dr. BOUGRINE Mohammed djamel for serving as my committee members. I would especially like to thank everyone helps me to get this work accomplished.

I would also like to thank my family. Words cannot express how grateful I am to my Parents for all of the sacrifices that they have made on my behalf. Their prayer and support for me were what sustained me thus far. I am equally thankful to my siblings, whose encouragement and understanding throughout this journey have been invaluable. I would also like to thank all of my friends who supported me in preparing my thesis, and incented me to strive towards my goal.

Special thanks to LACoSERE laboratory members. Their support and benefic discussions make the way to accomplish this work easy.

MENNAD Meriem
Laghouat University
June 2024

Dedication

To my beloved family, whose unwavering support and encouragement have been my greatest strength throughout this journey.

To my parents, for their endless love, sacrifices, and belief in me; to my sisters and brother, for their constant support and inspiration.

To my friends, for their constant companionship and encouragement.

To everyone who did not hesitate to extend a helping hand to me, this achievement would not have been possible without each of you.

I dedicate my humble work to you.

Liste of Abbreviations

Abbreviation	**Description**
AC	Alternative Current
c_1, c_2	Acceleration coefficients (personal and collective learning factor)
DC	Direct Current
DC-AC converter	Direct Current to Alternative Current converter
DC-DC converter	Direct Current to Direct Current converter
d	Duty cycle
dmin	Minimal distance between MPPs
GP	Global peak
GPV	Grid-Connected Photovoltaic
GMPP	Global Maximum Power Point
Gb	Global best
Gbp	Global best position
I-V	Current versus Voltage
In	Last monitored current
Irr	Irradiance
i	PV cell terminal current
i-PID	Intelligent Proportional Integral Derivative
iph	Photocurrent
is	Saturation current
K	Boltzmann's constant (1.381×10^{-23} J/K)
Ki	PID parameters
Kd	PID parameters
Kp	PID parameters
LP	Local peak
Lbp	Local best position

Abbreviation	**Description**
L_bi	Local best position of particle i
MFC	Model-Free control
MPPT	Maximum Power Point Tracking
MPP	Maximum Power Point
n	Number of bypass diodes
P-V	Power versus Voltage
PID	Proportional Integral Derivative
PI	Proportional Integral
pi	Best personal position
pg	Best global position
PSC	Partial Shading Conditions
P&O	Perturb and Observe
PV	PhotoVoltaic
PVG	Photovoltaic Generator
Pmpp	Maximum power point power
q	Electron charge (1.602×10^{-19} C)
r1, r2	Random numbers between 0 and 1
Rsh	Cell shunt resistance
Rp	Cell shunt resistance (assuming duplicate entry)
Rs	Cell series resistance
SISO	Single Input Single Output
T	Temperature
UIC	Uniform Irradiance Condition
Vn	Last monitored voltage
Vmin	The lowest possible voltage value
Vref	The reference voltage
Vupdated	The updated voltage
vi	Velocity of particle i
xi	Position

Contents

Abstract i

Acknowledgements ii

Dedication iii

Liste of Abbreviations v

List of Figures x

General Introduction xi

1 Fundamentals of Photovoltaic Energy 1

1.1 Introduction 1

1.2 The principle of photovoltaic energy operation 2

1.3 Solar Cell Equivalent Circuit and Electrical Equations 3

1.4 Photovoltaic (PV) panels 4

1.5 Our PV Panel Parameters 5

1.6 The PVG with MPPT control 6

1.7 Perturb and Observe (P&O) 8

1.8 Partial Shading Condition (PSC) 9

1.9 P&O Algorithm with a Checking Algorithm 11

1.10 Conclusion 14

2 PSO and MFC 15

2.1 Introduction 15

2.2 PARTICLE SWARM OPTIMIZATION (PSO) BASED MPPT 17
2.2.1 Introduction to Optimization and Swarm Intelligence 17
2.2.2 Fundamentals and Dynamics of Particle Swarm Optimization (PSO) . 17
2.2.3 Essential Components and Effectiveness of PSO 19
2.2.4 PSO Methodology in Optimizing Dynamic Systems 19
2.2.5 Flowchart of Particle Swarm Optimization (PSO) 20
2.2.6 PSO Algorithm for MPPT in Photovoltaic Systems 22
2.3 MODEL-FREE CONTROL 24
2.3.1 General principles 24
2.3.2 The ultra-local model 24
2.3.3 Intelligent PID controllers 25
2.3.4 Numerical value of β 26
2.3.5 A first academic example: a stable single-variable linear system 26
2.4 MPPT Using MFC Control 28
2.4.1 Implementing Model-Free Control (MFC) for Maximum Power Point Tracking (MPPT) on a PV System 28
2.4.2 Integration of PSO and MFC in a Photovoltaic System 29
2.4.3 Enhancing MPPT Efficiency with PSO and MFC on a PV System . . 30
2.5 Conclusion 31

3 Stimulation and Results **32**
3.1 Introduction 32
3.2 Tracking MPP using P&O method and PI controller 33
3.3 Tracking MPP using P&O method and Model-Free control 38
3.4 Tracking MPP using PSO method and PID controller 39
3.5 Tracking MPP using PSO method and Model-Free control 45
3.6 Comparative Analysis 47
3.6.1 P&O with PI Regulation vs. P&O with MFC 47
3.6.2 PSO with PID Regulation vs. PSO with MFC 47
3.6.3 PID Regulation vs. Model-Free Control (MFC) 48
3.7 Conclusion 49

General Conclusion **50**

List of Figures

1.1 The principle of photovoltaic energy operation.[8] 3
1.2 Equivalent circuit diagram of a solar cell.[1] 4
1.4 I(V) and P(V) characteristic of our PV array 6
1.5 PVG-load connection through a DC/DC converter and MPPT control.[7] . . 7
1.6 Principle of operation for the perturb and observe (P&O) algorithm.[15] . . . 8
1.7 Flowchart of P&O algorithm.[17] 9
1.8 (a) PV string at uniform irradiance condition, (b–d) PV string under partial shading conditions.[10] 10
1.9 P–V characteristics curve for uniform and partial shading.[10] 11
1.10 P-V Curve under Partial Shading with P&O Algorithm.[3] 12
1.11 Flow Chart of P&O with Checking Algorithm.[3] 13
1.12 P-V Curve under Partial Shading with Adapted P&O Algorithm and Checking Algorithm.[3] 13

2.1 Bird flocks.[12] 17
2.2 Graphical illustration of the basic PSO algorithm. 18
2.3 A graphic depiction of the tension between the global best and the particle best in determining the new particle position. 19
2.4 illustrates the flowchart of PSO.[16] 21
2.5 How a standard PSO algorithm scan the P–V curve of a photovoltaic (PV) module to find global maximum power point (GMPP).[4] 23
2.6 Stable linear single-variable system (Output (–); reference (- -); denoised output (. .)).[11] 28

2.7 Photovoltaic system with Particle Swarm Optimization (PSO) and Model-Free Control (MFC). 29

3.1 The functional diagram of the PI control 35
3.2 Simulation of P&O with PI. 36
3.3 Irradiances conditions (W/m2). 36
3.4 P-V characteristics curve. 36
3.5 Results of P&O with PI. 37
3.6 Simulation of P&O with MFC. 38
3.7 Results of P&O with MFC. 38
3.8 PV voltage regulation.[13] 40
3.9 Irradiance conditions (1). 42
3.10 Irradiance conditions (2). 42
3.11 Irradiance conditions (3). 42
3.12 Irradiance conditions (4). 43
3.13 Simulation of PSO with PID. 43
3.14 Results of PSO with PID. 44
3.15 Simulation of PSO with MFC. 45
3.16 Results of PSO with MFC. 46

General Introduction

The transition to renewable energy sources is a crucial step in addressing the growing global energy demand and mitigating the adverse effects of climate change. Among various renewable energy technologies, photovoltaic (PV) systems have emerged as a viable and sustainable solution due to their ability to directly convert sunlight into electricity. However, maximizing the efficiency and reliability of PV systems remains a significant challenge, especially under varying environmental conditions such as partial shading.

This project explores advanced techniques for optimizing the performance of PV systems through sophisticated Maximum Power Point Tracking (MPPT) algorithms and control strategies. Specifically, it investigates the efficacy of the Perturb and Observe (P&O) and Particle Swarm Optimization (PSO) methods, both in conjunction with Proportional-Integral (PI) controllers and Model-Free Control (MFC). The objective is to enhance both the precision of MPPT and the stability of the PV system, thereby improving overall energy capture and system reliability.

This master thesis is divided on three chapters besides the introduction and the conclusion:

- **In chapter one**, the fundamental principles of photovoltaic energy are discussed, providing a foundational understanding of the operation of solar cells and the application of MPPT techniques. The Perturb and Observe (PO) algorithm, a widely recognized MPPT technique, serves as the foundation for this investigation. Despite its simplicity and ease of implementation, PO is often hindered by its susceptibility to local maxima under PSC. To address these limitations, this thesis integrates a checking algorithm with PO, demonstrating its potential to maximize power output amidst dynamic environmental changes.

- **The second chapter** explores advanced control strategies, with a particular focus on Particle Swarm Optimization (PSO) and Model-Free Control (MFC). PSO, inspired by the social behavior of bird flocking, emerges as a robust optimization method capable of efficiently identifying the Global Maximum Power Point (GMPP) in complex and dynamic PV systems. Meanwhile, MFC introduces innovative approaches using intelligent PID controllers and Ultra-Local Models, providing adaptive MPPT solutions without relying on explicit system models. The synergy between PSO and MFC represents a significant advancement in MPPT technology. By combining PSO's global optimization capabilities with MFC's adaptive, model-free nature, this thesis presents a novel approach to overcoming the challenges posed by PSC and other dynamic conditions in PV systems.

- **In the third chapter** extends these concepts by presenting a detailed simulation study of a PV system integrating PSO and MFC for MPPT control. The simulation results validate the effectiveness of these integrated strategies, highlighting their potential to enhance the reliability and efficiency of PV energy harvesting. The study underscores the superiority of the combined PSO and MFC approaches in maximizing power extraction under diverse operating conditions, thereby improving the overall performance of PV systems.

The research is structured to provide a comprehensive analysis of each MPPT method and control strategy, followed by detailed simulations and results. The findings from these studies offer valuable insights into the strengths and limitations of each approach, guiding future research and development in the PV domain. By integrating advanced control mechanisms with GMPPT techniques like Flatness Control, this thesis aims to contribute to the optimization of PV systems, ensuring their effective deployment in diverse and challenging environments.

Chapter 1

Fundamentals of Photovoltaic Energy

1.1 Introduction

The rapid evolution of photovoltaic (PV) technology has positioned solar energy as a crucial player in the global transition towards sustainable and renewable energy sources. This chapter delves into the intricate workings and principles underlying the operation of photovoltaic energy systems, laying a strong foundation for understanding the nuances of this transformative technology.

First and foremost, the chapter illuminates the core principles governing photovoltaic energy operation. It elucidates the photovoltaic effect, wherein semiconductor materials within PV panels convert sunlight into electricity through the generation of electron-hole pairs. This fundamental process underscores the remarkable potential of solar energy as a clean and abundant resource.

Central to the discussion are PV panels themselves, the heart of solar energy systems. Detailed exploration is undertaken into the construction, materials, and functioning of PV panels, highlighting their role as the primary energy conversion devices in photovoltaic systems. Additionally, the chapter delves into the electrical equations and characteristics governing PV panels, providing a comprehensive understanding of their performance metrics and operational parameters.

A pivotal advancement in maximizing the efficiency and output of PV systems is the integration of Maximum Power Point Tracking (MPPT) control. The chapter delves into Grid-Connected Photovoltaic (GPV) systems equipped with MPPT technology, emphasizing its critical role in optimizing energy production by dynamically tracking the maximum power

point of PV panels under varying environmental conditions.

Within the realm of MPPT algorithms, particular focus is directed towards the Perturb and Observe (P&O) algorithm, a widely utilized method for MPPT control. The chapter delves into the intricacies of the P&O algorithm, its algorithms, and mechanisms for effectively tracking the maximum power point of PV panels, thus enhancing energy yield and system performance.

Moreover, the chapter addresses the challenge of Partial Shading Conditions (PSC), a common occurrence that can significantly impact the efficiency of PV systems. Strategies for mitigating the adverse effects of partial shading, including adaptations of the P&O algorithm and the incorporation of a Checking Algorithm, are discussed in detail. These approaches are crucial for ensuring optimal MPPT performance and maximizing energy generation even in complex shading scenarios.

Through a meticulous exploration of these topics, this chapter aims to provide a comprehensive and authoritative guide to the design, operation, and management of high-performance photovoltaic energy systems. It serves as a valuable resource for researchers, engineers, and practitioners seeking to harness the full potential of solar energy in meeting the world's growing energy demands sustainably and efficiently.

1.2 The principle of photovoltaic energy operation

Photovoltaic cells convert sunlight into electricity, A photovoltaic (PV) cell, commonly called a solar cell, is a non-mechanical device that converts sunlight directly into electricity. Some PV cells can convert artificial light into electricity.

Sunlight is composed of photons, or particles of solar energy. These photons contain varying amounts of energy that correspond to the different wavelengths of the solar spectrum.

A PV cell is made of semiconductor material. When photons strike a PV cell, they may reflect off the cell, pass through the cell, or be absorbed by the semiconductor material. Only the absorbed photons provide energy to generate electricity. When the semiconductor material absorbs enough sunlight (solar energy), electrons are dislodged from the material's atoms. Special treatment of the material surface during manufacturing makes the front surface of the cell more receptive to the dislodged, or free, electrons so that the electrons naturally migrate to the surface of the cell.

The flow of electricity in a solar cell, the movement of electrons, each carrying a negative

charge, toward the front surface of the solar photovoltaic cell creates an imbalance of electrical charge between the cell's front and back surfaces. This imbalance, in turn, creates a voltage potential like the negative and positive terminals of a battery. Electrical conductors on the cell absorb the electrons. When the conductors are connected in an electrical circuit to an external load, such as a battery, electricity flows through the circuit [8].

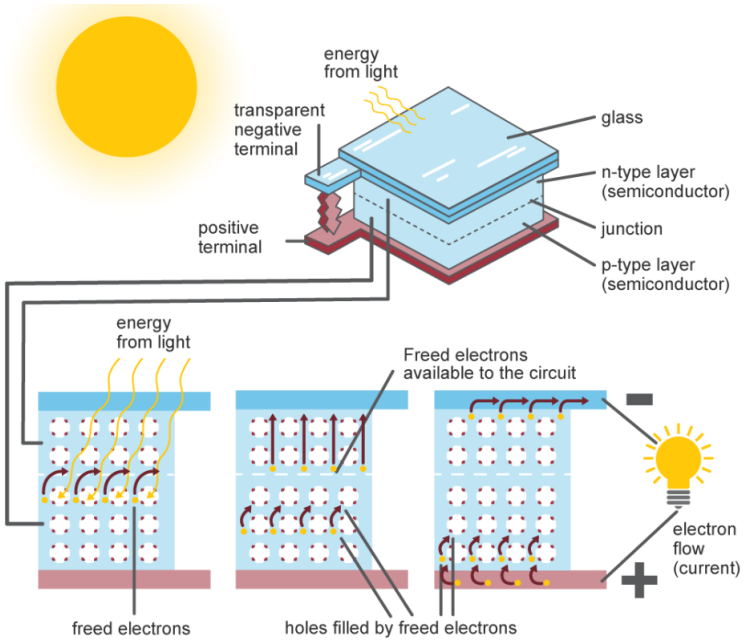

Figure 1.1: The principle of photovoltaic energy operation.[8]

1.3 Solar Cell Equivalent Circuit and Electrical Equations

An equivalent circuit model presents a theoretical circuit diagram, which captures the electrical characteristics of a device. It is important to note the components illustrated in the model are not physically present in the devices themselves. Instead, these models serve to help us visualize and simplify calculations related to the cell's behaviour. These models are invaluable for understanding fundamental device physics, explaining specific phenomena, and aiding in the design of more efficient devices.

The equivalent circuit of a solar cell consists of an ideal current generator in parallel with a diode in reverse bias, both of which are connected to a load. The generated current is directly proportional to light intensity. This highlights how important it is to accurately replicate

the solar spectrum when testing solar cells, and why solar simulators are an indispensable piece of equipment in this context. Although the amount of current produced varies with light intensity, there are other limitations in solar cells which cap their efficiency. These limitations are represented by the other components in the circuit [1].

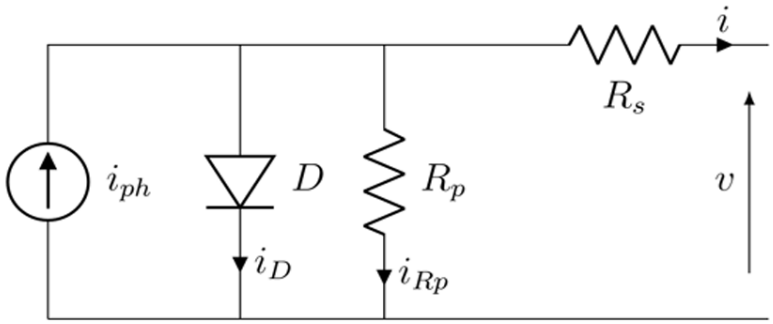

Figure 1.2: Equivalent circuit diagram of a solar cell.[1]

Parallel to this ideal current generator is a diode. The power that can be extracted from a device (P) is equal to current (I) times by voltage (V):

$$P = V \times I \tag{1.1}$$

Current-Voltage Relation (I-V Characteristic): The current-voltage relationship in a photovoltaic cell is governed by the Shockley diode equation:

$$I = I_{\text{ph}} - I_s \left(\exp \left[\frac{qV}{nkT} \right] - 1 \right) \tag{1.2}$$

where I is the current, $I_p h$ is the photo-current, I_s is the saturation current, q is the charge of an electron, V is the voltage, k is Boltzmann's constant, and T is the temperature in Kelvin .

Power-Voltage Relation (P-V Characteristic):

The power-voltage relationship in a photovoltaic cell is given by:

$$P = V \times I_{\text{ph}} - I_s \left(\exp \left[\frac{qV}{nkT} \right] - 1 \right) \tag{1.3}$$

1.4 Photovoltaic (PV) panels

A PV panel is a group of interconnected PV cells that convert sunlight directly into electrical energy through the photovoltaic effect. Each PV cell consists of semiconductor materials, such

as silicon, that generate an electric current when exposed to sunlight. The PV cells within a panel are typically arranged in a series and parallel configuration to achieve the desired voltage and current levels. In a series configuration, PV cells are connected end-to-end to add their voltages, while in parallel (shunt), they are connected side-by-side to increase the current capacity. This arrangement optimizes the panel's performance under varying sunlight conditions. When sunlight strikes the PV panel, photons in the sunlight excite electrons within the semiconductor material, creating an electric current. This generated electricity can be used immediately, stored in batteries, or fed into the electrical grid through inverters for wider distribution and consumption.

(a) solar panels.[18]

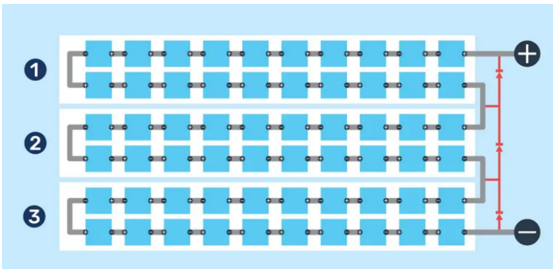

(b) solar cells.[14]

1.5 Our PV Panel Parameters

- Maximum Power (W): 85.204 W
- Open Circuit Voltage (Voc): 22.1 V
- Voltage at Maximum Power Point (Vmp): 17.9 V
- Temperature Coefficient of Voc: $-0.36901\%/C$
- Cells per Module (Ncell): 32
- Short-Circuit Current (Isc): 5.02 A
- Current at Maximum Power Point (Imp): 4.76 A
- Temperature Coefficient of Isc: 0.086998%/C

the I-V and P-V characteristics

The I(V) characteristic of a photovoltaic cell illustrates the relationship between current and voltage under varying sunlight intensities and temperatures. It exhibits a nonlinear

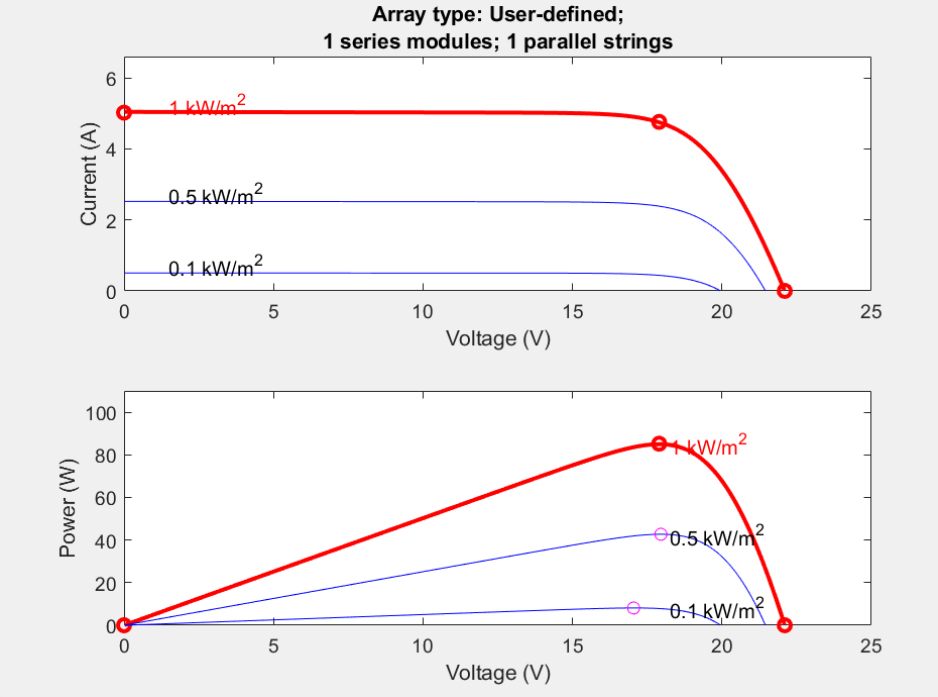

Figure 1.4: I(V) and P(V) characteristic of our PV array

behaviour, with a peak corresponding to the maximum power point (MPP) where the cell operates most efficiently.

The P(V) characteristic graphically represents the power output of the cell at different voltage levels. It highlights the MPP where the product of voltage and current is maximized, indicating the optimal operating conditions for the cell.

1.6 The PVG with MPPT control

Solar panels, although becoming increasingly efficient, still have relatively low yields. This is why it's crucial to maximize the power they can generate while minimizing energy losses. The maximum power of these panels corresponds to a single operating point called the Maximum Power Point (MPP). This point primarily depends on insolation, temperature, and load variations that change over time. Implementing a Maximum Power Point Tracking (MPPT) algorithm is necessary to find this point. The challenge lies in searching for the MPP while ensuring a perfect match between the generator and its load to transfer the maximum power.[5]

To simplify the operation of this control, a DC load is often chosen. As depicted in this chain, the MPPT control is necessarily associated with a quadrupole possessing degrees of freedom to enable adaptation between the PV system and the load. In the case of solar

conversion, the quadrupole can be realized using a DC-DC converter so that the power supplied by the PV system corresponds to its maximum power output, which can then be transferred directly to the load.[5]

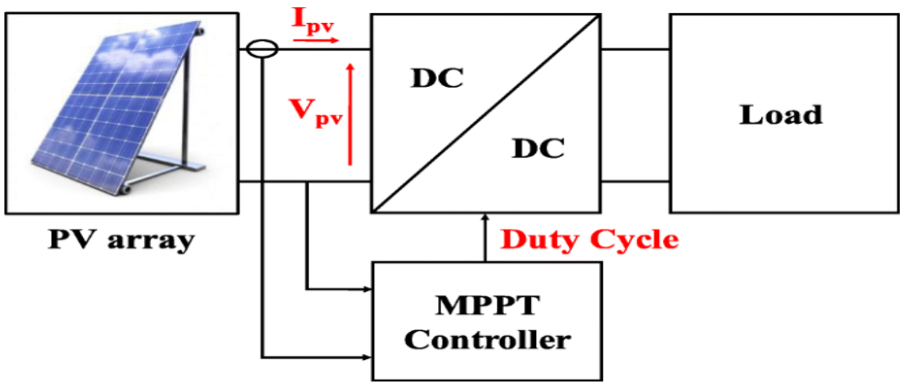

Figure 1.5: PVG-load connection through a DC/DC converter and MPPT control.[7]

The commonly used control technique involves automatically adjusting the duty cycle to bring the generator to its optimal operating value, regardless of meteorological instabilities or sudden load variations that may occur at any time.

In summary, Global Maximum Power Point Tracking (GMPPT) is achieved through a specific control mechanism that primarily manipulates the duty cycle of the static converter to locate and reach the Maximum Power Point (MPP) of the PV system. Several algorithms have been implemented to search for the maximum power point. [5]

1.7 Perturb and Observe (P&O)

The P&O algorithm has been selected to track MPP of the PV array due to its simplicity and ease of implementation. P&O is initiated by applying a perturbed voltage (dV), to alter the operating voltage of the PV array. [17]

Even though the optimal operating voltage is successfully identified, P&O algorithm will continuously iterate the operating voltage with the aim to track the next MPP. As a result, the perturbation process will lead to the voltage and power fluctuation issues. The fluctuation is obvious when a large perturbation size is applied. By optimizing the perturbation size of dV, the oscillation of the PV operating voltage is anticipated to be minimum hence reducing power loss in the PV system. [17]

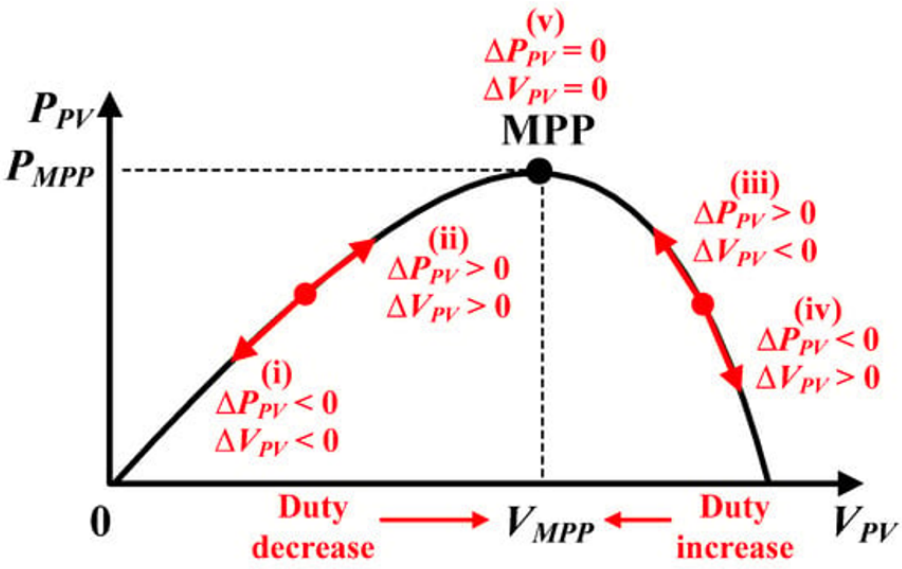

Figure 1.6: Principle of operation for the perturb and observe (P&O) algorithm.[15]

The change of output power at the present and the previous sampling interval are subsequently compared. Based on the instantaneous output power of the two sampling intervals, the algorithm will decide to regulate the PV array to be operated either at larger or lower operating voltage. The PV array will pursue numerous iteration processes but eventually the PV system will operate at a particular optimum power point. At this stage, PV array will be generating maximum output power. The tracking principal of P&O algorithm is illustrated in Figure 1.7.[17]

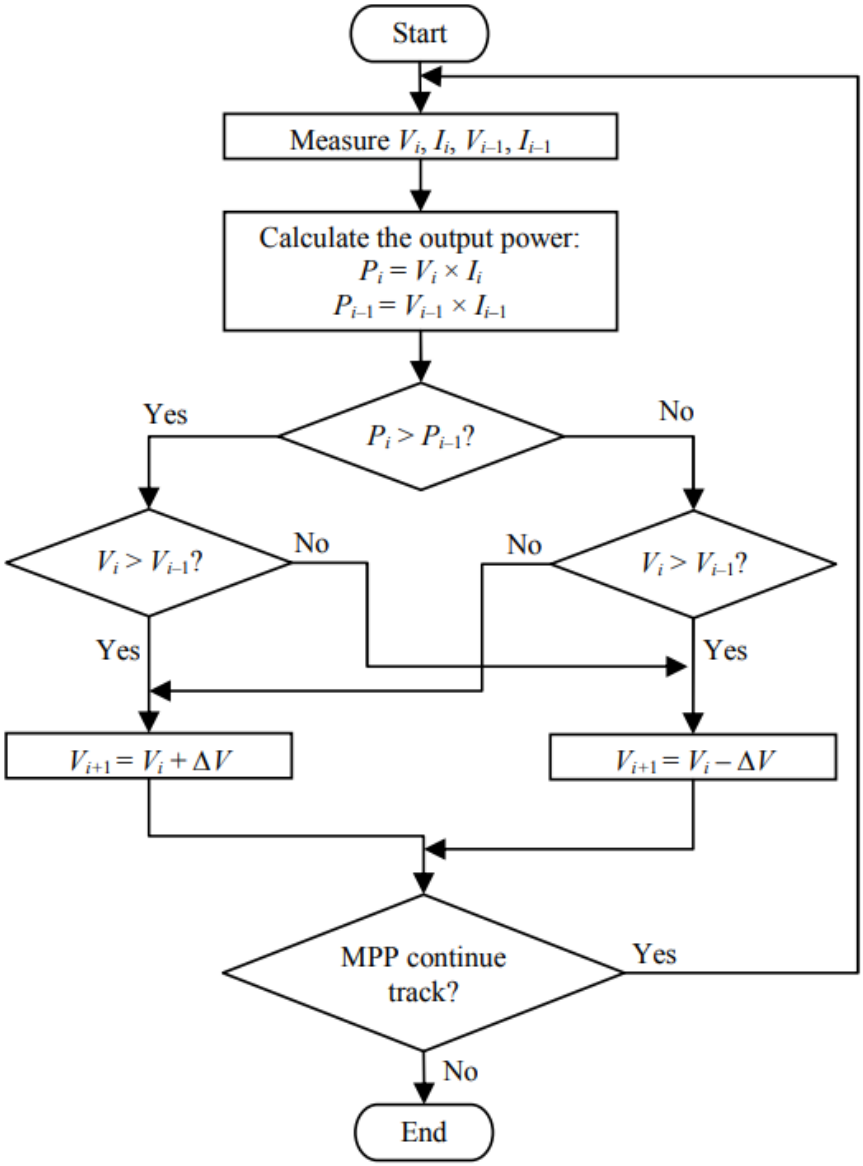

Figure 1.7: Flowchart of P&O algorithm.[17]

1.8 Partial Shading Condition (PSC)

A single PV cell can produce a few watts of electricity. Thus, multiple PV cells are connected in series and parallel configurations to form a PV module. However, a PV string consists of multiple PV modules connected in series. While a PV array consists of multiple PV strings connected in a parallel configuration. PSC is a phenomenon at which some part of the PV module is receiving different irradiance level as compared to other parts. Thus, in a string, a shaded module will produce low current. However, in a series-connected PV system, current

should remain constant, but, in this case, the shaded module will work in a reverse biased condition, and it will drop a huge amount of voltage across Rp.[10]

Thus, it produces a hotspot at that point and sometimes it will damage the PV module. Thus, to reduce the huge power loss due to PSC, a bypass diode is used to avoid the shaded module. The bypass diode is normally used to minimize the adverse effect of the shaded module, and the voltage drop across the bypass diode is just 0.7 V. Figure 1.8. depicts the PSC. The PV string shown in Figure 1.8.(a) represents a uniform irradiance condition (UIC).[10]

However, Figure 1.8.(b–d) represent PV strings with different irradiance levels i.e., PSC. Under (UIC), all the solar module works as a current source, and all diodes work in reverse biased conditions. However, under PSC, the shaded solar cells act as an open circuit. Thus, the total current flow throws the internal resistance Rp, which produces a huge voltage loss. In order to avoid this voltage-drop, the bypass diode works in a forward biased condition, and the solar cell is completely bypassed. Thus, the voltage drop would be just 0.7 V [10]

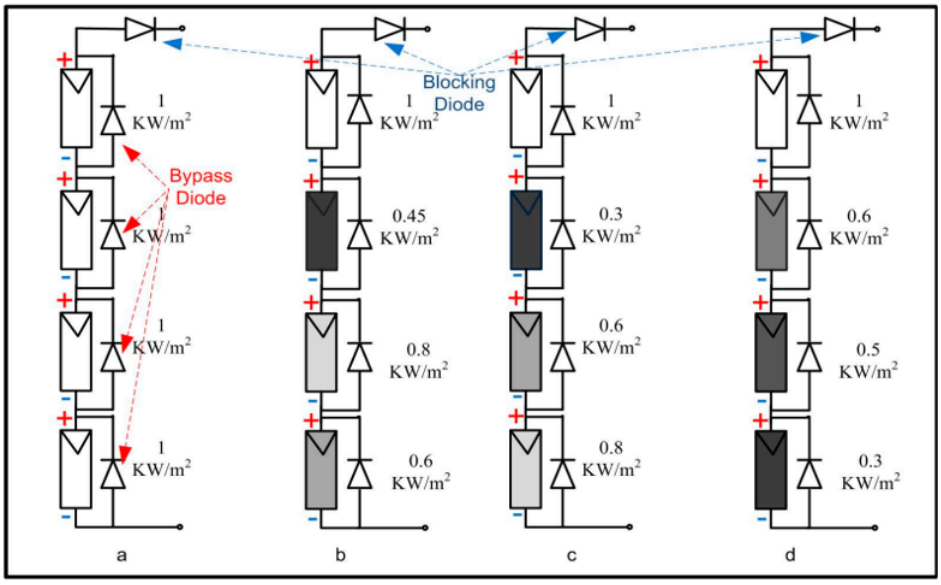

Figure 1.8: (a) PV string at uniform irradiance condition, (b–d) PV string under partial shading conditions.[10]

The PV string with different irradiance condition is shown in Figure 1.8. The power vs. voltage (P-V) curve of the PV string subjected to multiple PSC is illustrated in Figure 1.9. The curve in blue with a single maximum peak at 800 W corresponds to a UIC. However, the remaining curve illustrates PSC. Thus, Figure 1.9. shows that multiple peaks appear in the P-V curves during partial shading conditions. However, there is a single MPP that

appears in each curve, which is known as global peak (GP), and remaining peaks are known as local peak (LP). Furthermore, in UIC, there is just one GP and no LP. However, under PSC, there are many LPs but only a single GP. Thus, to detect the GP from all existing peaks, an accurate and robust tracking technique is required and that is known as Maximum Power Point Tracking (MPPT). The MPPT becomes more complex and challenging with the variation in temperature and irradiance. For example, in Figure 1.9, the light blue line indicates UIC, but, due to the PSC case, multiple peaks are produced in the remaining curves. The shading curves have GP at 800 W, 613 W, 528 W, 406 W, 397 W, and 330 W. Similarly, the voltage at GP is between 80 V to 120 V.[10]

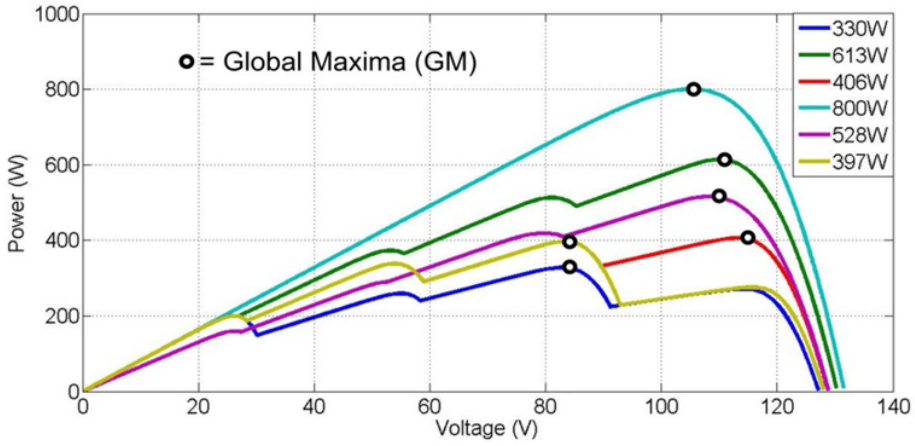

Figure 1.9: P–V characteristics curve for uniform and partial shading.[10]

1.9 P&O Algorithm with a Checking Algorithm

The main idea of the P&O method is to track the maximum power point algorithm. However, Figure 1.10. shows the(P-V) Curve under the Partial Shading Conditions, where the conventional P&O algorithm is, indicating that one peak point has been reached and tracked. Yet, it is still unable to track the global MPP which usually gets confused and trapped at the local MPP as shown in Figure 1.10. Therefore, the algorithm needs to be modified again in order to ensure the algorithm is tracking the real MPP.[3]

Partial Shading with PandO

The checking algorithm Figure 1.11 is added after the variable step size of P&O MPPT to determine whether the saved MMP is the global MPP or only a local MPP. A few concrete operating points need to be measured and compared with the saved MPP. Equation 1.4

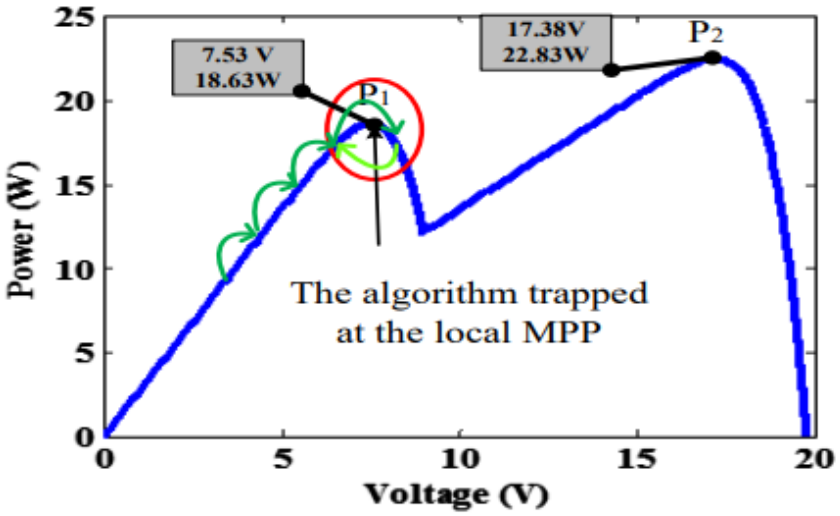

Figure 1.10: P-V Curve under Partial Shading with P&O Algorithm.[3]

calculates the approximation of minimal distance between MPPs in order to ensure whether it would have to sense to look for another MPP in the surrounding area of the already known operating point.[3]

$$d_{\min} = \frac{V_{\max}}{n} \tag{1.4}$$

where Vmax = nearest voltage to the open circuit voltage, n = number of bypass diode The checking algorithm starts with reference voltage, Vn set from the lowest possible voltage value, Vmin. Thus, another operating point that needs to be measured is the nearest voltage to the short circuit current. Once voltage and current are monitored, the power is calculated and compared with the saved MPP. If it is greater, the voltage will be updated with the reference voltage (Vupdated = Vn). Oppositely, a new operating point is calculated. [3]

$$V_{n+1} = \frac{P_{\text{mpp}}}{I_n} \tag{1.5}$$

where Pmpp = maximum power point power obtained by the previous 'P&O subroutine', In = last monitored current.

Next, the new operating point is measured and compared again with the saved MPP value. These steps are repeated to find the highest peak point. In other words, the whole curve will be continuously scanned. The tracking process will be changing abruptly to the possible highest peak point existed as presented in Figure 1.12. The MPP values would be updated and once again, the variable step size of P&O algorithm takes place to determine

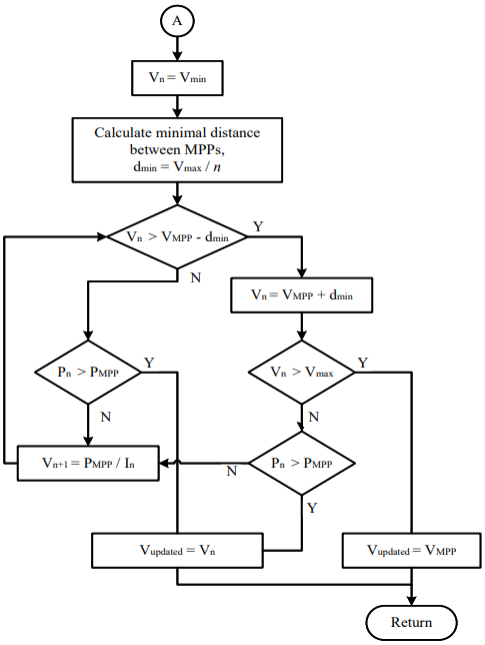

Figure 1.11: Flow Chart of P&O with Checking Algorithm.[3]

the most accurate value for MPP.[3]

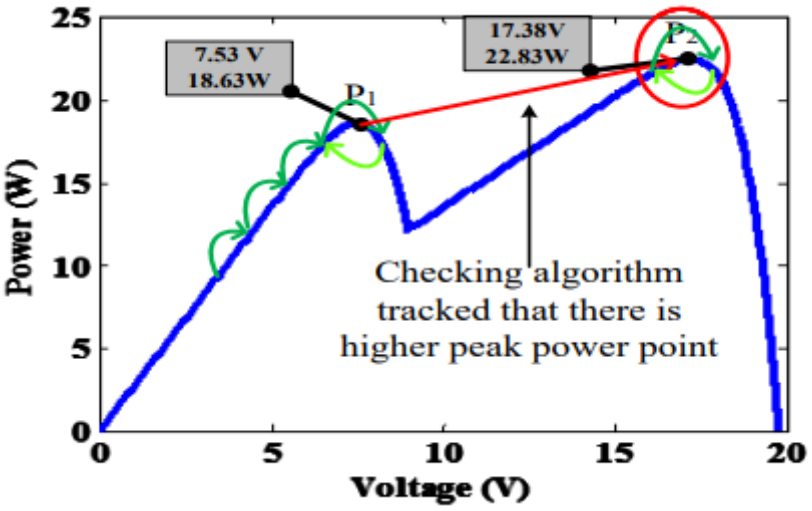

Figure 1.12: P-V Curve under Partial Shading with Adapted P&O Algorithm and Checking Algorithm.[3]

Maximizing the energy output of solar panels is crucial for efficient solar power systems, especially under partial shading conditions. While traditional MPPT (Maximum Power Point Tracking) algorithms like the Perturb and Observe (P&O) method have been widely used,

they often struggle to handle partial shading scenarios effectively. On the other hand, the Particle Swarm Optimization (PSO) algorithm offers significant advantages, particularly in dealing with partial shading conditions. PSO excels at quickly finding the optimal solution without being trapped in local maxima, leading to improved accuracy and efficiency in tracking the maximum power point of solar panels even in partially shaded environments. In the next chapter, we will explore the mechanics and benefits of PSO algorithm in depth, highlighting why PSO is a superior choice for MPPT in solar energy systems, especially when dealing with partial shading challenges.[3]

1.10 Conclusion

this chapter has provided a comprehensive exploration of the principles, components, and optimization techniques within photovoltaic (PV) energy systems. We have delved into the fundamental operation of PV panels, understanding their electrical equations and characteristics, and highlighting the crucial role they play in converting sunlight into clean electricity. The integration of Maximum Power Point Tracking (MPPT) control, particularly through the Perturb and Observe (P&O) algorithm, has been examined as a key strategy for enhancing energy yield and system efficiency in Photovoltaic Generator (PVG) systems.

Moreover, we have addressed the challenges posed by Partial Shading Conditions (PSC) and discussed strategies such as adaptations of the P&O algorithm and the utilization of Checking Algorithms to mitigate their impact and ensure optimal MPPT performance.

Looking ahead, the next chapter will delve deeper into optimization techniques for MPPT, with a particular focus on the Particle Swarm Optimization (PSO) algorithm and Model-Free Control (MFC). We will explore how PSO and MFC offer advantages over traditional algorithms like P&O, and how they contribute to further enhancing the efficiency and performance of PV energy systems. By continuing to advance our understanding and implementation of these optimization strategies, we move closer to unlocking the full potential of solar energy as a sustainable and impactful renewable energy source.

Chapter 2

Particle Swarm Optimisation(PSO) and Model-Free Control (MFC)

2.1 Introduction

In the pursuit of optimizing the performance of photovoltaic (PV) systems, the quest for efficient Maximum Power Point Tracking (MPPT) methodologies remains at the forefront of research and development. This chapter delves into the exploration of two cutting-edge approaches, Particle Swarm Optimization (PSO) and Model-Free Control (MFC), each offering unique insights and strategies to enhance MPPT efficiency and reliability.

The journey begins with an in-depth examination of Particle Swarm Optimization (PSO) in the context of MPPT. Through a comprehensive exploration of its fundamentals, dynamics, and essential components, readers are introduced to the underlying principles of swarm intelligence and its application in optimizing dynamic systems. The elucidation of PSO methodology, coupled with a detailed analysis of its flowchart and practical applications, sets the stage for understanding its pivotal role in locating the Global Maximum Power Point (GMPP) on a PV module under partial shading conditions.

Transitioning seamlessly to the realm of Model-Free Control (MFC), the chapter embarks on a journey into the realm of control strategies devoid of complex mathematical models. From the elucidation of general principles to the intricacies of the ultra-local model and the numerical value of β, readers are guided through the development of intelligent PID controllers within the MFC framework. Through a first academic example and numerical simulations, the versatility and efficacy of MFC in stable mono-variable linear systems are

vividly showcased.

The convergence of PSO and MFC emerges as a transformative strategy for enhancing MPPT efficiency in PV systems. As the chapter progresses, readers are introduced to the seamless integration of these methodologies, unlocking unprecedented opportunities to optimize power extraction, adapt to dynamic environmental conditions, and bolster system stability. Through practical examples and real-world applications, the chapter illuminates the synergistic potential of PSO and MFC in revolutionizing MPPT strategies for PV systems.

2.2 PARTICLE SWARM OPTIMIZATION (PSO) BASED MPPT

2.2.1 Introduction to Optimization and Swarm Intelligence

Optimization is a branch of mathematics that solves problems by determining the best element from a set according to predefined criteria. As such, optimization is ubiquitous across all domains and has been evolving continuously since Euclid. Optimization techniques inspired by swarm intelligence have become increasingly popular in the past decade. They are characterized by a decentralized working method that mimics the behaviour of insect societies, bird flocks Figure 2.1, or schools of fish. The advantage of these approaches over traditional techniques lies in their flexibility. These properties make swarm intelligence an example of successful design for algorithms that tackle increasingly complex problems. In this chapter, we focus on one of these intelligent optimization methods: Particle Swarm Optimization (PSO). This is the technique we will use to determine the maximum power point in the presence of shading issues.[6]

Figure 2.1: Bird flocks.[12]

2.2.2 Fundamentals and Dynamics of Particle Swarm Optimization (PSO)

Particle Swarm Optimization (PSO) was introduced in 1995 by Russel Eberhart, an electrical engineer, and James Kennedy, a social psychologist. This method is based on collaboration among individuals: Each particle is defined by its position (a solution) and its velocity. In PSO optimization, the velocity of each particle is iteratively modified based on its best

personal position and the best position found by particles in its neighbourhood. Consequently, each particle explores around a region defined by its best personal position and the best position in its neighbourhood. From now on, we use (V_i) to denote the velocity of the (ith) particle in the swarm, (x_i) to denote its position, (p_i) to denote its best personal position, and (p_g) to denote the best global position found by particles in their neighbourhoods.

Many real-world optimization problems are dynamic and require optimization algorithms capable of adapting to optimal evolution over time. For instance, traffic conditions in a city change dynamically and continuously. What might be considered an optimal route at one moment may not be optimal the next minute. Unlike optimization towards a static optimum, in a dynamic environment, the goal is to replicate the optimal dynamic evolution as closely as possible.

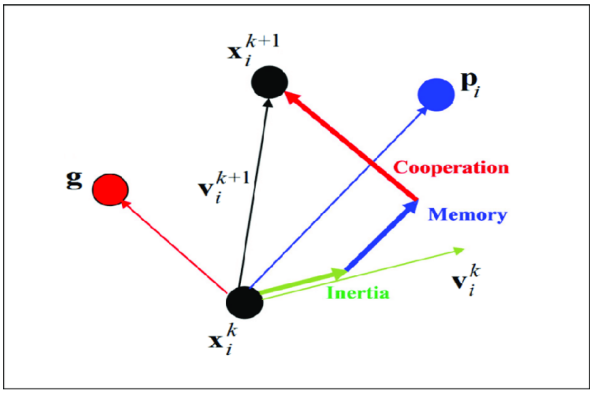

Figure 2.2: Graphical illustration of the basic PSO algorithm.

2.2.3 Essential Components and Effectiveness of PSO

Particle Swarm Optimization (PSO) has two main ingredients: particle dynamics and the particle information network. Particle dynamics stem from swarm simulations in computer graphics, while the information-sharing component is inspired by social networks. These ingredients make PSO a robust and efficient optimizer of real objective functions (although PSO has also been successfully applied to combinatorial and discrete problems).

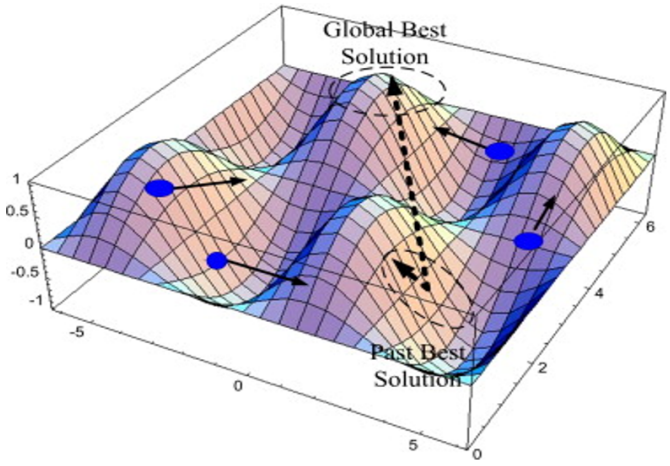

Figure 2.3: A graphic depiction of the tension between the global best and the particle best in determining the new particle position.

2.2.4 PSO Methodology in Optimizing Dynamic Systems

The PSO method is a stochastic optimization technique inspired by the behaviours of bird flocking together in a surrounding with little idea to search for food, PSO is a computational acumen method that solves a problem optimally by emulating a flock searching over the search space for solution. [9]

In this paper, the particles of PSO are referred to the potential perturbation sizes of P&O. This algorithm allows all the random particles to search for the optimum solution in the search space through iterative process. Each particle will learn their best experience while interacting with each other to share their intellectual information.[9]

Two rules are followed during the learning process of particles; attraction towards the global best position (Gbp) discovered by others (collective influence) and drawn towards its local best capable position (Lbp) (personal influence). The position of each particle will be

evaluated by a fitness function. In this work, the fitness function utilizes the output voltage, V and output current, I to calculate the fitness value (output power) of each particle. The Gbp and Lbp are defined by the amount of power generated by a specific operating voltage. The highest power generated is the best. All through the searching process, the velocity and position of each particle is updated based on the inertia, collective component and personal component,[9], as shown in (2.1) and (2.2):

$$V_(i+1) = V_i + c_1 r_1 (L_b i - x_i) + c_2 r_2 (G_b - x_i) \tag{2.1}$$

$$x_(i+1) = x_i + (tv)_(i+1) \tag{2.2}$$

Where:

- V_i: velocity of particle i,
- c_1 and c_2: acceleration coefficients (personal and collective learning factor),
- r_1 and r_2: random numbers between 0 and 1,
- L_{bi}: local best position of particle i,
- G_b: global best position,
- x_i: current position of particle i respectively.

2.2.5 Flowchart of Particle Swarm Optimization (PSO)

The PSO searching process will be terminated when the maximum number of iterations is fulfilled. Figure 2.4. illustrates the flowchart of PSO.[9]

- Step 1: The process begins.
- Step 2: Initialize the variables V_i (velocity) and x_i (position).
- Step 3: Calculate the fitness of the position x_i. Fitness evaluation is typically a function that measures how good the solution represented by x_i is.
- Step 4: Update the local best (LB) and global best (GB) positions based on the fitness evaluations. LB refers to the best solution found by a particular particle, while GB is the best solution found by any particle in the swarm.

- Step 5: Update the velocity V_i and position x_i of the particle. This step involves adjusting the trajectory of the particle based on its own experience (LB) and the experience of others (GB).
- Step 6: Re-evaluate the fitness of the new position x_i after the updates.
- Step 7: Check if the number of particles evaluated equals the maximum number allowed. This is a loop condition to ensure that all particles are processed.
- Step 8: Determine if the stopping criteria of the algorithm are met. This could be a maximum number of iterations, a satisfactory fitness level, or other algorithm-specific conditions.
- Step 9: Once the stopping criteria are fulfilled, finalize the process by obtaining the optimized perturbation size. This refers to the final adjustments or the best solution found by the algorithm.

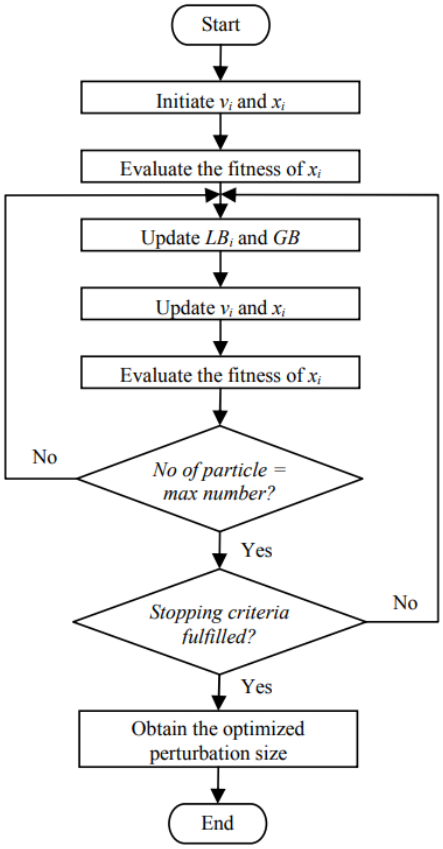

Figure 2.4: illustrates the flowchart of PSO.[16]

2.2.6 PSO Algorithm for MPPT in Photovoltaic Systems

the Figure 2.5 present the implementing of PSO, In the context of implementing PSO for Global Maximum Power Point Tracking (GMPPT) in a photovoltaic (PV) system simulation, we define the following terms:

- **Position (Xi)**: Represents the voltage applied to the PV array or module.
- **Velocity (Vi)**: Represents how much the voltage (Xi) changes over time (iterations).
- **Fitness**: Represents the objective function evaluated based on the power output of the PV system at a given voltage (Xi).

Steps in PV PSO Implementation

1. **Initialization**:
   - Initialize a swarm of particles with random positions (Xi) and velocities (Vi).
2. **Objective Function (Fitness Evaluation)**:
   - For each particle, compute the fitness based on the power output of the PV system at the voltage (Xi).
   - Use the PV module's current-voltage (I-V) characteristics or its P-V curve to calculate power output (P = V . I)
   - Adjust for current environmental conditions like irradiance and temperature.
3. **Updating Velocities and Positions**:
   - Update each particle's velocity (Vi) and position (Xi) based on:
     - Inertia: Maintaining the current velocity to some extent.
     - Cognitive Component: Moving towards the best position (pBest) the particle has achieved.
     - Social Component: Moving towards the best position (gBest) found by any particle in the swarm.
4. **Iterative Optimization**:
   - Repeat the velocity and position updates for a specified number of iterations or until convergence (when changes in fitness or position become negligible).

5. **Output**:

   - The global best position (gBest) after the iterations represents the optimal voltage (Vref) that maximizes the power output (Pmpp) of the PV system under current environmental conditions.

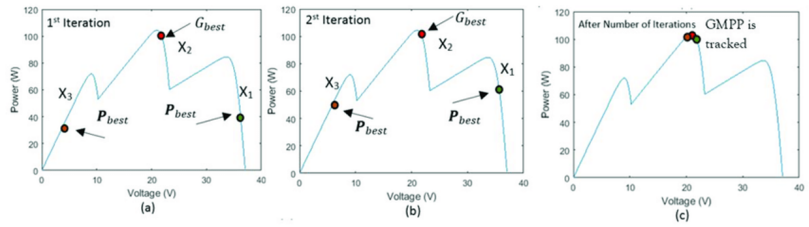

Figure 2.5: How a standard PSO algorithm scan the P–V curve of a photovoltaic (PV) module to find global maximum power point (GMPP).[4]

2.3 MODEL-FREE CONTROL

Model-Free Control (MFC) is a control strategy that does not rely on a mathematical model of the system it aims to regulate. Instead, MFC utilizes real-time data and simple algorithms to adjust control actions dynamically. This approach continuously updates the controller based on the observed input-output behaviour, making it adaptable to varying system conditions. Unlike traditional methods requiring complex system identification and modeling, MFC simplifies the control process. It is particularly advantageous in environments where the system dynamics are complex or poorly understood. MFC's flexibility and ease of implementation make it suitable for a wide range of applications. This approach ensures robust performance despite changes in system dynamics and external disturbances.

2.3.1 General principles

Model-free control relies on continuous local modeling based solely on the observed input/output behaviour. It differs from "black box" identification methods commonly found in literature which seek a valid model over the widest possible operating range. The MFC control and its corresponding "intelligent" PID controllers provide a controller that is continuously updated based on the dynamic changes of the entire system (including its load). The entire converter is modeled as a reduced-order localized model, which is defined only for a short duration and requires no identification procedure[11].

2.3.2 The ultra-local model

Let us now summarize some of the main theoretical ideas which are shaping our model-free control. We restrict ourselves for simplicity's sake to systems with a single control variable u and a single output variable y. The unknown "complex" mathematical model is replaced by an ultra-local model[11]

$$y^{(n)} = F + \beta u \tag{2.3}$$

Where

- $y^{(\nu)}$ is the derivative of order $\nu \geq 1$ of y. The integer ν is selected by the practitioner. The existing examples show that ν may always be chosen quite low, i.e., 1, or, only seldom, 2.

- $\beta \in \mathbb{R}$ is a non-physical constant parameter, such that F and βu are of the same magnitude;
- the numerical value of F, which contains the whole "structural information", is determined thanks to the knowledge of u, β, and of the estimate of the derivative $y^{(n)}$.

In all the numerous known examples it was possible to set n=1 or 2 .

We only assume that the plant behaviour is well approximated in its operational range by a system of ordinary differential equations, which might be highly nonlinear and time-varying. The system, which is SISO, may be therefore described by the input-output equation

$$E(t, y, \dot{y}, \ldots, y^{(l)}, u, \dot{u}, \ldots, u^{(k)}) = 0 \tag{2.4}$$

where

- u and y are the input and output variables,
- E, which might be unknown, is assumed to be a sufficiently smooth function of its arguments.

Assume that for some integer n,$(n,\ 0 < n \leq l,\ \frac{\partial E}{\partial y^{(n)}} \neq 0)$. From the implicit function theorem, we may write locally

$$y^{(n)} = E\left(t, y, \dot{y}, \ldots, y^{(n-1)}, y^{(n+1)}, \ldots, y^{(l)}, u, \dot{u}, \ldots, u^{(k)}\right) \tag{2.5}$$

2.3.3 Intelligent PID controllers

Generalities: If n=1, we close the loop via the intelligent PI controller, or i-PI controller[11],

$$u = -\frac{F}{\beta} + \frac{\dot{y}^*}{\beta} + K_P e + K_I \int e\, dt \tag{2.6}$$

where

- $\dot{y}^*$ is the output reference trajectory, which is determined via the rules of flatness-based control;
- $e = y^* - y$ is the tracking error;
- K_P, K_I are the usual tuning gains.

The i-PI controller is compensating the poorly known term F. Controlling the system therefore boils down to the control of a precise and elementary pure integrator. The tuning of the gains KP and KI becomes therefore quite straightforward[11]. Assume that n=2 in Equation (2.3):

$$\ddot{y}^{(n)} = F + \beta u \tag{2.7}$$

Close the loop via the intelligent proportional-integral derivative controller, or iPID,

$$u = \frac{F - \ddot{y}^* + K_P e + K_I \int e\, dt + K_D \dot{e}}{\beta} \tag{2.8}$$

where

- y^* is the reference trajectory,
- $e = y - y^*$ is the tracking error,
- K_P, K_I, K_D are the usual tuning gains.

2.3.4 Numerical value of β

Let us emphasize that one only needs to give an approximate numerical value to β. It would be meaningless to refer to a precise value of this parameter[11].

2.3.5 A first academic example: a stable single-variable linear system

the stable transfer function:

$$\frac{(S+2)^2}{(S+1)^3} \tag{2.9}$$

A classic PID controller:

We apply the well-known method due to Broïda, by approximating System 2.9 via the following delay system [11]

$$\frac{Ke^{-\tau s}}{Ts+1} \tag{2.10}$$

$$K = 4,\ T = 2.018,\ \tau = 0.2424$$

are obtained thanks to graphical techniques. The gain of the PID controller are then deduced:

$$K_P = \frac{100(0.4\tau + T)}{120K\tau} = 1.8181, K_I = 11.33K\tau = 0.7754, K_D = \frac{0.35T}{K} = 0.1766 \quad (2.11)$$

I-PI:

We are employing

$$y^* = F + u \quad (2.12)$$

and the i-PI controller

$$u = -[F]_e + \dot{y}^* + PI(e) \quad (2.13)$$

where

- $F_e = [\dot{y}]_e - u$,
- y^* is a reference trajectory,
- $e = y^* - y$,
- $PI(e)$ is a usual PI controller.

Numerical simulations:

Figure 2.6(a) shows that the i-PI controller behaves only slightly better than the classic PID controller (Figure 2.6(b)). When taking into account on the other hand the ageing process and some fault accommodation there is a dramatic change of situation: Figure 2.6(c) indicates a clear-cut superiority of our i-PI controller if the ageing process corresponds to a shift of the pole from 1 to 1.5, and if the previous graphical identification is not repeated (Figure 2.6(d))[11].

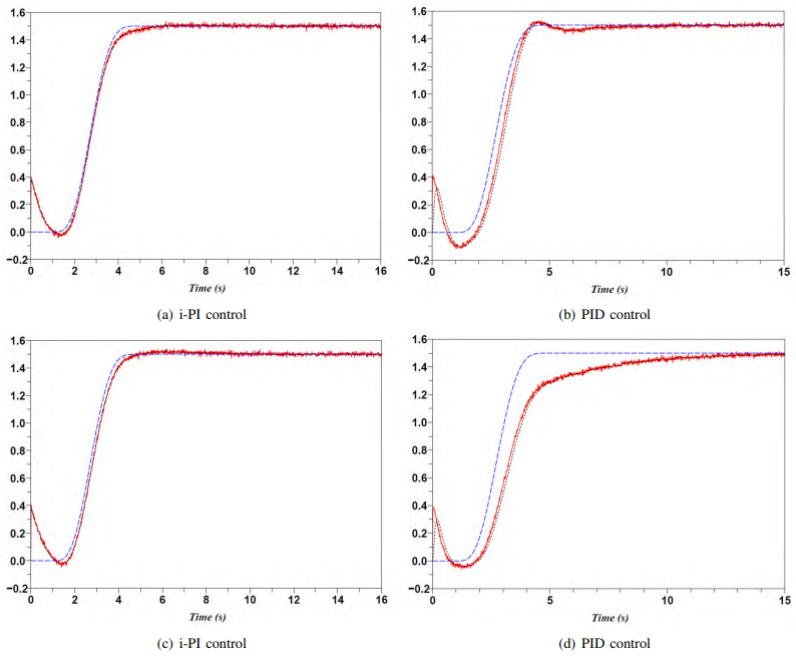

Figure 2.6: Stable linear single-variable system (Output (–); reference (- -); denoised output (. .)).[11]

2.4 MPPT Using MFC Control

2.4.1 Implementing Model-Free Control (MFC) for Maximum Power Point Tracking (MPPT) on a PV System

In this section, we apply MFC control for the MPPT tracking of a PVG. We implement MFC on the same system studied in previous sections.

In the general case, our system can be described by equation (2.4) where u is the input to the converter and y is the voltage delivered by the PVG. The proposed control strategy replaces the mathematical model of the converter, including the load, with a "phenomenological" model, valid only for a short period of time. For the k-th iteration, the local model F is defined as follows:

$$y^{(v)} = F_{k-1} + \beta u_{k-1} \tag{2.14}$$

where β is a design constant that is not physically based. F is estimated at each iteration based on the knowledge of β, u, and $\dot{y}$. Equation (2.14) guides us to provide an "intelligent"

digital PI controller, which is of the form.

$$u_k = -\frac{1}{\beta}\left(F_{k-1} - \left|y^{(*^{(v)})}\right|_k\right) + |c(y^* - y)|_k \tag{2.15}$$

- c: is a corrector, generally a PID controller.
- $\dot{y}$: is the desired output.

We replace (2.14) in (2.15) the command u becomes:

$$u_k = u_{k-1} - \frac{1}{\beta}\left(\left|y^{(v)}\right|_{k-1} - \left|y^{(*^{(v)})}\right|_k\right) + |c(y^* - y)|_k \tag{2.16}$$

2.4.2 Integration of PSO and MFC in a Photovoltaic System

Consider the system with boost converter (Figure 2.7) where u is the duty cycle:

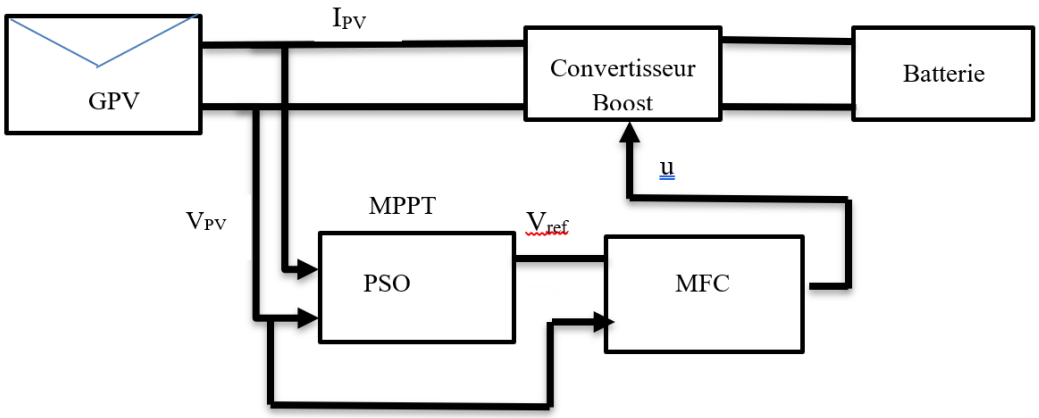

Figure 2.7: Photovoltaic system with Particle Swarm Optimization (PSO) and Model-Free Control (MFC).

In our case $y = v_{\text{pv}}$ and $y^* = v_{\text{ref}}$.

So, equation (2.16) will be as follows:

$$u_k = u_{k-1} - \frac{1}{\beta}\left(\left|v_{\text{pv}}^{(v)}\right|_{k-1} - \left|v_{\text{ref}}^{(*^{(v)})}\right|_k\right) + |c(v_{\text{ref}}^* - v_{\text{pv}})|_k \tag{2.17}$$

2.4.3 Enhancing MPPT Efficiency with PSO and MFC on a PV System

Implementing Particle Swarm Optimization (PSO) and Model-Free Control (MFC) methods on a PV system enhances the efficiency and reliability of maximum power point tracking (MPPT) under varying environmental conditions. PSO leverages swarm intelligence to optimize the PV system's output by dynamically adjusting the duty cycles of the DC-DC converter to find the global maximum power point (GMPP). Meanwhile, MFC provides robust control by directly regulating the output without relying on a detailed mathematical model, making it highly adaptive to changes in irradiation and temperature. Together, these methods ensure optimal power extraction and improve the overall performance and stability of the PV system. The detailed results of this implementation will be presented in the next chapter.

2.5 Conclusion

In conclusion, this chapter has explored advanced techniques for Maximum Power Point Tracking (MPPT) in photovoltaic (PV) systems, focusing on Particle Swarm Optimization (PSO) and Model-Free Control (MFC). Through a comprehensive examination of PSO's optimization principles and MFC's model-free approach, we have uncovered innovative strategies to enhance MPPT efficiency and reliability in renewable energy applications.

Particle Swarm Optimization (PSO) has emerged as a powerful optimization technique, leveraging swarm intelligence to dynamically adjust PV system parameters and locate the Global Maximum Power Point (GMPP) under varying environmental conditions. By exploring its fundamentals, methodology, and practical applications, we have gained insights into its effectiveness in optimizing system outputs and overcoming challenges such as partial shading.

On the other hand, Model-Free Control (MFC) represents a paradigm shift in control strategies, offering robust solutions without relying on detailed mathematical models. Through the formulation of ultra-local models and the development of intelligent PID controllers, MFC demonstrates its versatility and adaptability in stabilizing PV system outputs and mitigating environmental uncertainties.

The integration of PSO and MFC presents a synergistic approach to MPPT, combining the strengths of optimization and control methodologies to enhance system performance and stability. By seamlessly integrating these advanced techniques, we unlock new opportunities to optimize power extraction, improve system efficiency, and ensure reliability in PV systems. As we look towards the future, further research and development in MPPT strategies hold the promise of advancing renewable energy technologies and accelerating the transition towards a sustainable energy future. By continuing to innovate and collaborate, we can harness the full potential of photovoltaic systems to meet the growing global energy demand while minimizing environmental impact.

Chapter 3

Stimulation and Results

3.1 Introduction

In the preceding chapters, we have established the theoretical foundations for tracking the Global Maximum Power Point (GMPP) in photovoltaic (PV) systems using Model-Free Control (MFC) and Particle Swarm Optimization (PSO).

This chapter aims to bridge the gap between theory and practice by presenting detailed simulations that validate the efficacy of the proposed methods. Through a series of carefully designed scenarios, we will demonstrate how the MFC and PSO algorithms work in tandem to optimize the power output of a PV system under various environmental conditions. These simulations are crucial for understanding the practical implications of our approach and for identifying potential areas for improvement.

We will begin by outlining the simulation setup, including the tools and parameters used. This will be followed by a detailed description of the implementation process for the control algorithms. Next, we will present the results from several case studies, each designed to test the system under different conditions such as varying irradiance levels and partial shading. The results will be analyzed to assess the performance of the MFC and PSO methods, comparing them with conventional MPPT techniques where applicable.

Finally, we will discuss the key findings, highlighting the strengths and weaknesses of our approach, and conclude with insights into the potential for future research and development in this area.

3.2 Tracking MPP using P&O method and PI controller

In figure (3.2) the simulation , we analyze the performance of a photovoltaic (PV) system utilizing the Perturb and Observe (P&O) method for Global Maximum Power Point Tracking (GMPPT) and a Proportional-Integral (PI) controller. The objective was to evaluate the effectiveness of the MPPT algorithm and the control strategy in optimizing the power output of the PV system. The simulation is conducted under the MATLAB/Simulink environment, and we chose the "Solar World module SW 85 W R5A" as the PV panel. The parameters of the photovoltaic panel studied are mentioned in the first chapter.

The used DC-DC Boost Averaged Model :

The averaging approach is based on the condition that the switching frequency is much higher than the system's critical dynamics, which are formed by energy-storage components: inductor and capacitor. Under this condition, the nonlinear switching dynamics can be neglected for dynamic analysis and controller design [13].

Over one switching cycle, the system equations can be derived from the on-state and off-state of the power switch.

Q on-state dynamics:

$$L\frac{di_L}{dt} = v_g - R_L i_L \tag{3.1}$$

$$C_1\frac{dv_g}{dt} = i_g - i_L = \frac{V_{eq} - v_g}{R_p} - i_L \tag{3.2}$$

Q off-state dynamics:

$$L\frac{di_L}{dt} = v_g - R_L i_L - (v_D + V_{bat}) \tag{3.3}$$

$$C_1\frac{dv_g}{dt} = i_g - i_L = \frac{V_{eq} - v_g}{R_p} - i_L \tag{3.4}$$

Averaging over one switching cycle:

$$L\frac{di_L}{dt} = v_g - R_L i_L - (v_D + V_{bat})(1-d) = v_g - R_L i_L - (v_D + V_{bat})d' \tag{3.5}$$

$$C_1\frac{dv_g}{dt} = \frac{V_{eq} - v_g}{R_p} - i_L \tag{3.6}$$

Where d is the duty cycle and $d' = (1-d)$ is the control variable.

Small-signal Model for Voltage Control

The objective of modeling the converter for voltage control is to obtain a small-signal transfer function that relates the small-signal voltage $\tilde{v}_g$ and the control variable $\tilde{d}'$. The modeling process is essentially composed of three steps: inserting the small-signal variables in the state equations, separating the dc and ac parts, applying the Laplace transformation, and manipulating the equations in order to find the desired transfer function. The small-signal variables are introduced with the following definitions:

$$\begin{cases} i_L = I_L + \tilde{i}_L \\ v_g = V_g + \tilde{v}_g \\ d' = D' + \tilde{d}' \end{cases} \tag{3.7}$$

Where DC steady state values are capitalized, and small signals are marked with a tilde.

Substituting 3.7 in equations 3.5 and 3.6 and taking only the ac parts, the small-signal model for the Boost converter will be like below:

$$L\frac{d\tilde{i}_L}{dt} = \tilde{v}_g - R_L\tilde{i}_L - (v_D + V_{bat})\tilde{d}' \tag{3.8}$$

$$C_1\frac{d\tilde{v}_g}{dt} = -\tilde{v}_g/R_p - \tilde{i}_L \tag{3.9}$$

Equations 3.10 and 3.11 show the state-space form of equations 3.9 and 3.8.

$$\frac{d}{dt}\begin{bmatrix}\tilde{i}_L \\ \tilde{v}_g\end{bmatrix} = \begin{bmatrix}-\frac{R_L}{L} & \frac{1}{L} \\ -\frac{1}{C_1} & \frac{1}{R_pC_1}\end{bmatrix}\begin{bmatrix}\tilde{i}_L \\ \tilde{v}_g\end{bmatrix} + \begin{bmatrix}-\frac{(v_D+V_{bat})}{L} \\ 0\end{bmatrix}\tilde{d}' \tag{3.10}$$

$$\tilde{y} = \begin{bmatrix}0 & 1\end{bmatrix}\begin{bmatrix}\tilde{i}_L \\ \tilde{v}_g\end{bmatrix} \tag{3.11}$$

Applying the Laplace transformation, the small-signal transfer function that relates the small-signal voltage $\tilde{v}_g$ and the control variable $\tilde{d}'$ is given as:

$$G_{vd}(s) = \frac{\tilde{v}_g}{\tilde{d}'} = \frac{K_{vd}}{s^2 + 2\xi_{vd}\omega_{vd}s + \omega_{vd}^2} \tag{3.12}$$

Where

$$K_{vd} = \frac{(v_D + V_{bat})}{LC_1} \tag{3.13}$$

$$\omega_{vd} = \sqrt{\frac{R_p - R_L}{LR_pC_1}} \tag{3.14}$$

$$\xi_{vd} = \frac{R_LR_pC_1 - L}{2LR_pC_1\omega_{vd}} \tag{3.15}$$

Numerical application: we calculated the optimal values of the inductance L and capacitor C_1 for a low ripple Δi_l and Δv_g. Next, we will define the parameters of the DC-DC Boost convertor.

Given:

$$v_D = 0.7\,\text{V} \quad ; \quad v_{bat} = 48\,\text{V} \quad ; \quad L = 600\,\mu\text{H} \quad ; \quad C_1 = 200\,\mu\text{F} \quad ; \quad R_l = 0.6\,\Omega \quad ; \quad R_p = 7.5\,\Omega$$

We used the irradiance conditions shown in Figure with a constant temperature $T = 25°\text{C}$.

For the application of a PI regulator to this system, we need a modeling of the latter in order to calculate the parameters of the PI regulator (K, T_i), which represent the proportional and integral actions, respectively[2]. Our regulator is applied to a 2^{nd} order system (DC/DC converter) described by the transfer function of the figure3.1 of the form:

$$G(p) = \frac{k_0\omega_0^2}{p^2 + 2\zeta\omega_0 p + \omega_0^2} \tag{3.16}$$

After solving our system, we determine the parameters of the regulator (K, T_i):

$$K = 0.0018 \quad \text{and} \quad T_i = 2.62$$

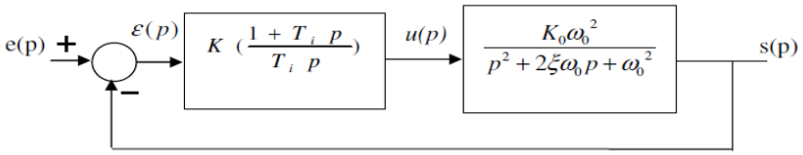

Figure 3.1: The functional diagram of the PI control

SIMULATIN

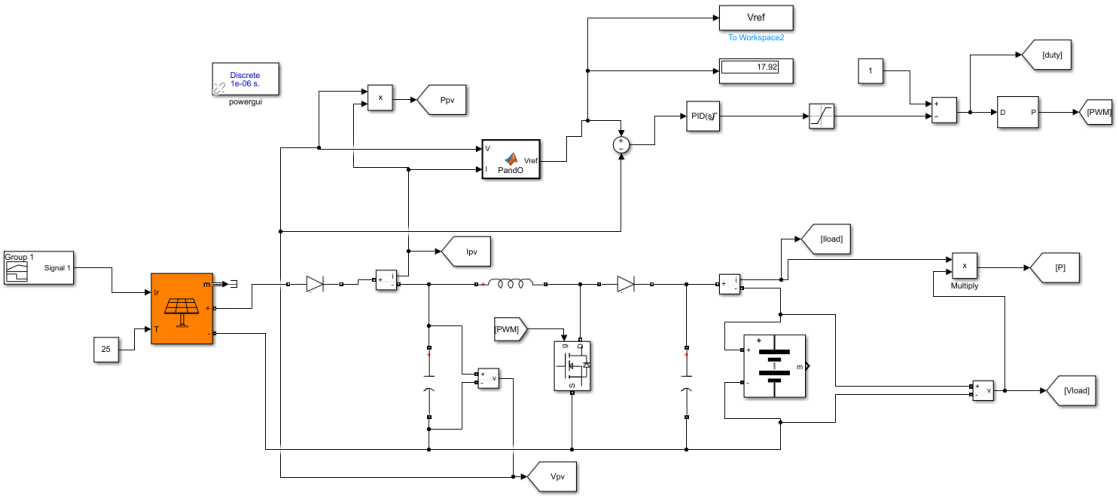

Figure 3.2: Simulation of P&O with PI.

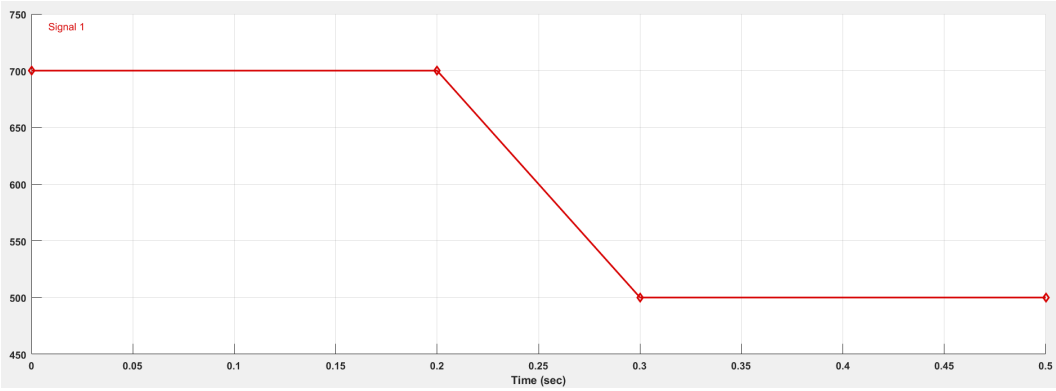

Figure 3.3: Irradiances conditions (W/m2).

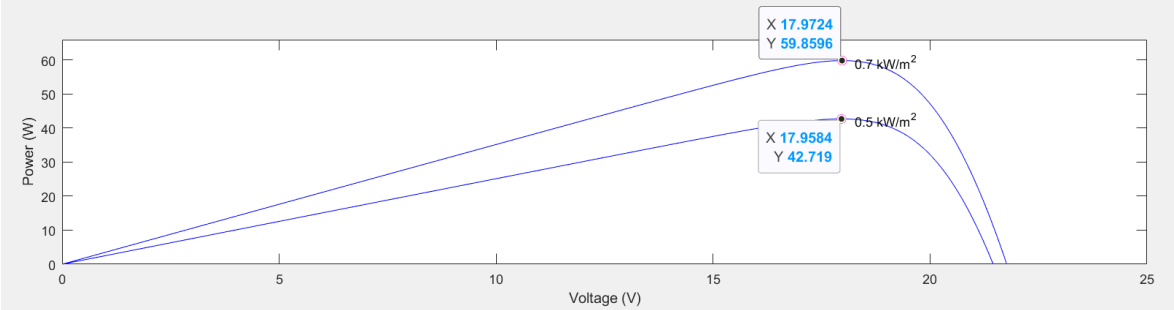

Figure 3.4: P-V characteristics curve.

RESULT

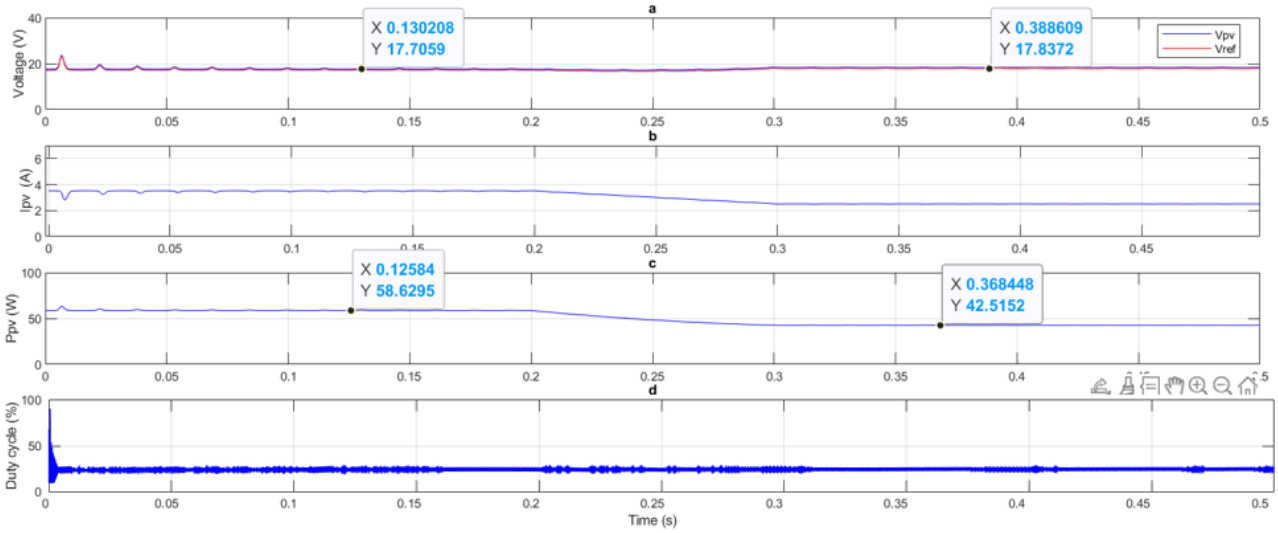

Figure 3.5: Results of P&O with PI.

Our simulation of a PV system using the P&O algorithm and PI regulation shows promising results under varying irradiance levels, as shown in the figure3.3. At an irradiance of 700 W/m², the system in the figure 3.4 shows that P_{mpp} is 59.8 W and V_{mpp} is 17.9 V, while the P&O and PI regulator achieved 58.6 W and V_{ref} at 17.7 V. At an irradiance of 500 W/m², the figure 3.4 shows that P_{mpp} is 42.7 W and V_{mpp} is 17.9 V, with the P&O and PI regulator results being 42.5 W and V_{ref} at 17.8 V. These results indicate the P&O algorithm's effectiveness in tracking the global maximum power point, despite slight discrepancies. However, the regulation from the PI controller is not as good because the voltage, power, and current curves have noticeable perturbations. Overall, the results demonstrate successful MPPT performance, with potential for further improvement in the PI regulation.

3.3 Tracking MPP using P&O method and Model-Free control

In this simulation , we are going to analyze the performance of a photovoltaic (PV) system using the Perturb and Observe (P&O) method for Maximum Power Point Tracking (MPPT) and a model-free control (MFC) strategy. The goal was to evaluate the effectiveness of these methods in optimizing the power output and maintaining the stability of the PV system. using the same conditions of the previous simulation.

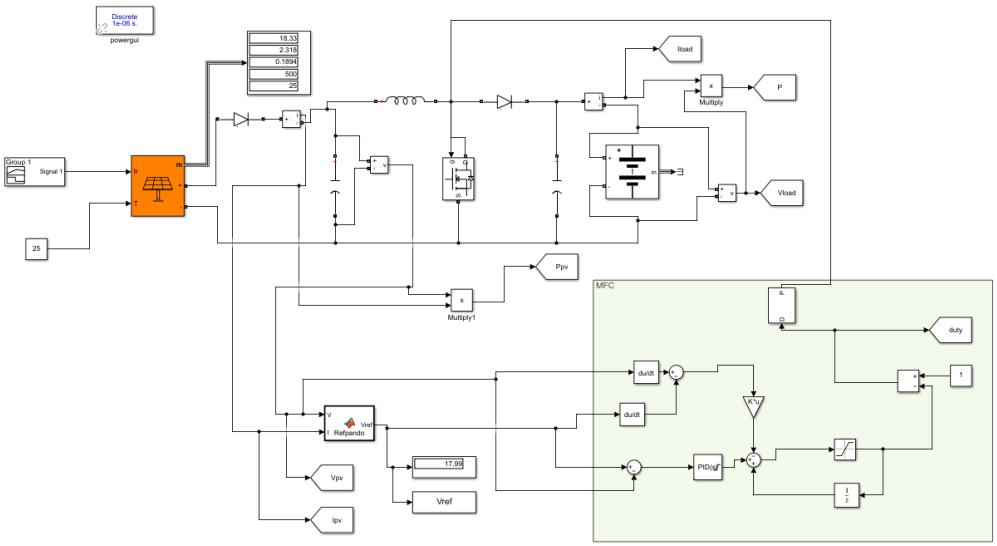

Figure 3.6: Simulation of P&O with MFC.

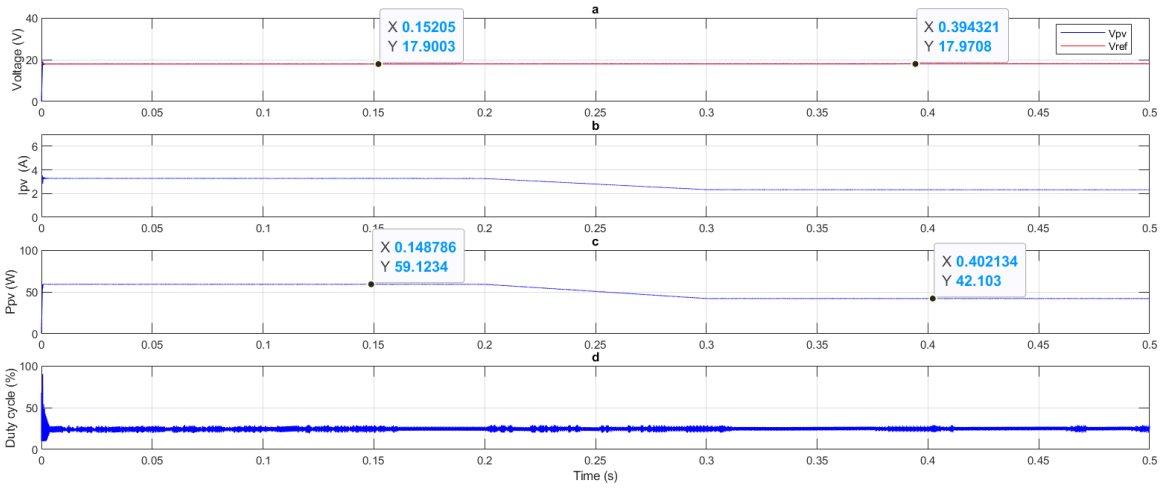

Figure 3.7: Results of P&O with MFC.

Based on the PV simulation in figure 3.6 using the P&O algorithm and Model-Free Control (MFC) under varying irradiance levels from 700 to 500 W/m², the results in the figure 3.7 show: at 700 W/m², P&O and MFC achieved a P_{mpp} of 59.1 W with V_{ref} maintained at 17.9 V, slightly below the simulated P_{mpp} of 59.8 W; at 500 W/m², P&O and MFC attained a P_{mpp} of 42.1 W with V_{ref} again at 17.9 V, compared to 42.7 W simulated. These outcomes demonstrate effective MPPT performance with close alignment between simulated and achieved power outputs. we see that the Vref stays at the same value 17.9 V When there is a change in irradiation in times (t=0.2s ;t=0.4s) and Notably, the absence of perturbations in voltage, power, and current curves underscores MFC's ability to enhance control stability and efficiency over traditional methods.

Building on these insights, our next simulations will focus on addressing the challenge of partial shading conditions in PV systems. Partial shading can significantly impact the performance and efficiency of PV systems by causing multiple local maxima in the power-voltage curve, making it difficult to accurately track the Gmpp using traditional methods like P&O.

To overcome this issue, we will implement Particle Swarm Optimization (PSO) as our MPPT technique. PSO is a robust optimization algorithm inspired by the social behavior of birds flocking, known for its effectiveness in finding the global optimum in complex, multi-modal functions.

3.4 Tracking MPP using PSO method and PID controller

In this study, we evaluate the performance of a photovoltaic (PV) system under partial shading conditions and under varying irradiance as the figures (fig(3.9), fig(3.10), fig(3.11), fig(3.12)) shows, using the Particle Swarm Optimization (PSO) method for Global Maximum Power Point Tracking (GMPPT) in conjunction with a Proportional-Integral Derivative (PID) controller. The goal is to assess the accuracy of the PSO method in tracking the global maximum power point (Gmpp) and the stability of the system. we are using the same PV panel type (SW85W) as the previous simulations.

Figure 3.8 shows the PV voltage regulation loop based on the mathematical model developed in the previous chapter. The controller regulates the PV link voltage to follow a

time-variant set point, which represents the voltage at the MPP (V_{MPP}). The MPP tracker continuously updates the value of V_{MPP}. Therefore, the regulation performance of the PV link voltage is essential for MPP tracking.[13]

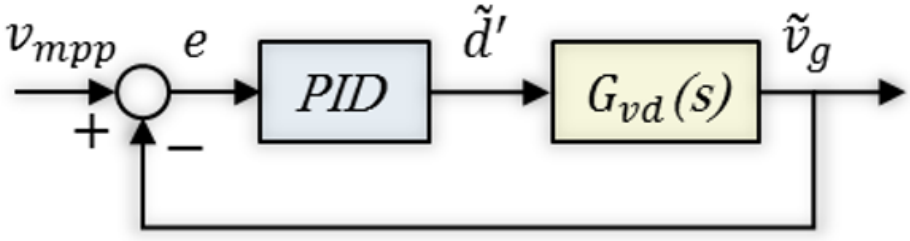

Figure 3.8: PV voltage regulation.[13]

Although more and more new control methods are being proposed for industrial applications, PID controllers appear as one of the most universally used controllers in the field of power electronics. They are based on a particular fixed structure. The combinations of proportional, integral, and derivative actions usually provide enough flexibility to design a linear controller with a stable loop control and the required performance.[13]

In Figure 3.8, the closed loop transfer function $T_0(s)$ is given by equation (3.17), where $G_{vd}(s)$ represents the nominal plant model (PV + Boost converter), $C(s)$ stands for the controller transfer function, $v_{\mathrm{mpp}}(s)$ is the control reference, $\tilde{d}'(s)$ symbolizes the control signal, and $\tilde{v}_g(s)$ is the plant output or the control variable.

The relationship between $T_0(s)$ and $C(s)$ is not proportional as shown in equation (3.17), causing the tuning of the controller parameters with respect to the required closed-loop performance to be unclear.

$$T_0(s) = \frac{\tilde{v}_g(s)}{v_{\mathrm{mpp}}(s)} = \frac{C(s)G_{vd}(s)}{1 + C(s)G_{vd}(s)} \tag{3.17}$$

Affine parameterization simplifies the model-based controller design by introducing a transfer function in terms of the variable $Q(s)$ as shown in equation (3.18).

$$\tilde{d}'(s) = Q(s)v_{\mathrm{mpp}}(s) \tag{3.18}$$

This simple transformation allows the transfer function of the closed-loop system to become as in equation (3.19). The transforming function between $Q(s)$ and $C(s)$ is obtained as in equation (3.20):

$$T_0(s) = \frac{\tilde{v}_g(s)}{v_{mpp}(s)} = Q(s)G_{vd}(s) \tag{3.19}$$

$$C(s) = \frac{Q(s)}{1 - Q(s)G_{vd}(s)} \tag{3.20}$$

In the studied system, G_{vd}, the desired closed-loop transfer function $F_Q(s)$ should be specified from both the damping ratio, which has a relation with the percentage of the overshoot, and the undamped natural frequency, which has a relation with the response speed, as in equation (3.21).

$$F_Q(s) = \frac{1}{\frac{1}{\omega_{cl}^2}s^2 + \frac{2\xi_{cl}}{\omega_{cl}}s + 1} = \frac{1}{\alpha_2 s^2 + \alpha_1 s + 1} \tag{3.21}$$

With the specified closed-loop parameters, the transfer function $Q(s)$ is derived as in equation (3.22). The function $Q(s)$ is stable, since the poles are the same as those in the predefined transfer function, $F_Q(s)$. Subsequently, the equivalent transfer function of the controller becomes as in equation (3.23).

$$Q(s) = F_Q(s)G_{vd}^{-1}(s) = \frac{s^2 + 2\xi_{vd}\omega_{vd}s + \omega_{vd}}{K_{vd}(\alpha_2 s^2 + \alpha_1 s + 1)} \tag{3.22}$$

$$C(s) = \frac{Q(s)}{1 - F_Q(s)} = \frac{s^2 + 2\xi_{vd}\omega_{vd}s + \omega_{vd}}{K_{vd}s(\alpha_2 s^2 + \alpha_1 s)} \tag{3.23}$$

It can be seen by analyzing equation (3.23) that the transfer function of the controller can also be expressed as an equivalent PID controller, in a parallel form as in equation (3.24).

$$C(s) = K_p + \frac{K_i}{s} + \frac{K_d s}{\tau_d s + 1} \tag{3.24}$$

Where the PID parameters can be derived as:

$$\tau_d = 1.7013 \times 10^{-5}$$

$$K_p = 0.0874$$

$$K_i = 640.3956$$

$$K_d = 4.3261 \times 10^{-6}$$

The following figures illustrate the irradiance conditions of the four pv panels. as follows:

- First PSC: $t = 0s$ to $t = 0.3s$

- Second PSC: $t = 0.3s$ to $t = 0.6s$
- Third PSC: $t = 0.6s$ to $t = 0.9s$

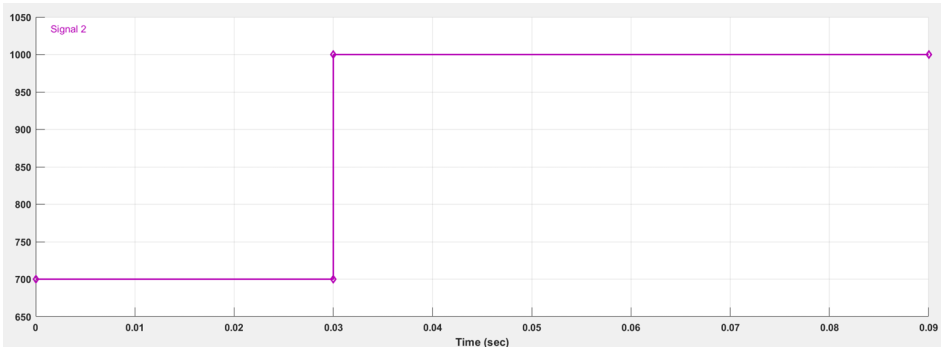

Figure 3.9: Irradiance conditions (1).

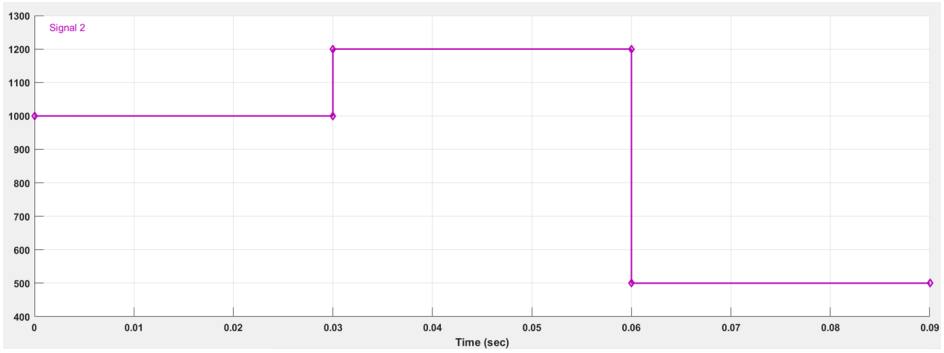

Figure 3.10: Irradiance conditions (2).

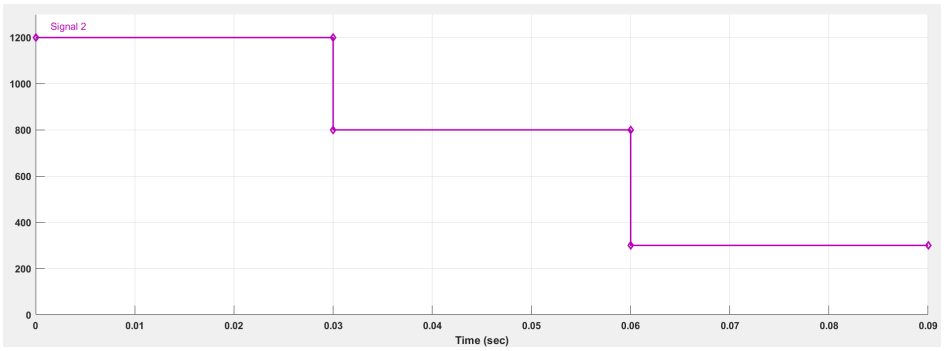

Figure 3.11: Irradiance conditions (3).

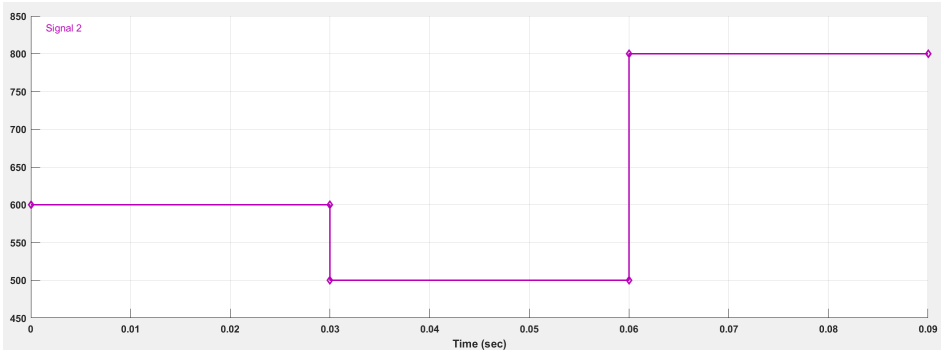

Figure 3.12: Irradiance conditions (4).

SIMULATION

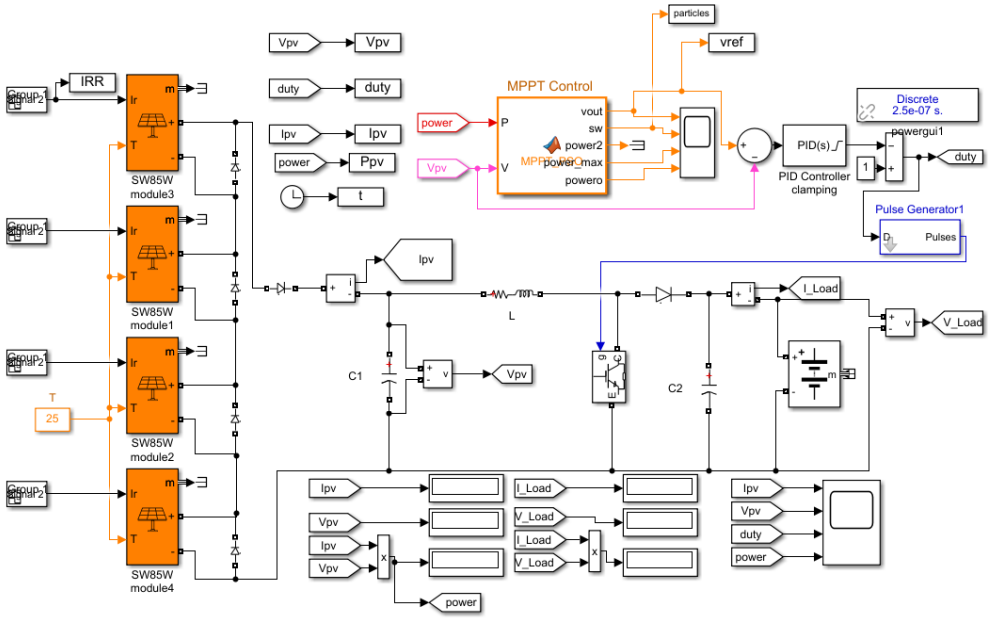

Figure 3.13: Simulation of PSO with PID.

RESULT

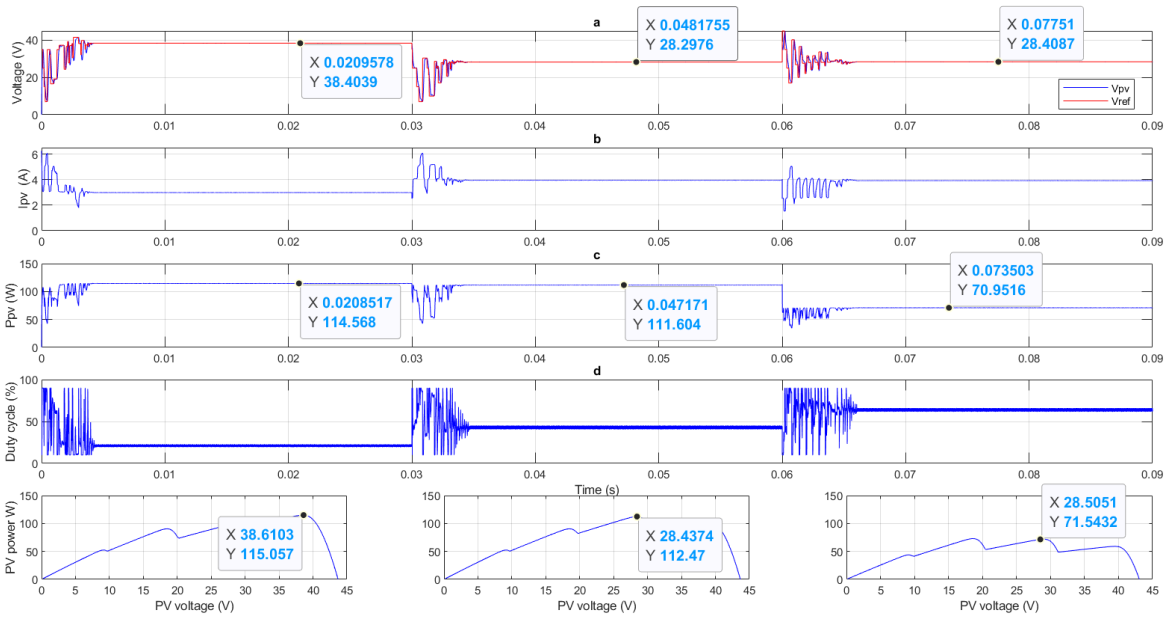

Figure 3.14: Results of PSO with PID.

Simulation Results:

1. First Partial Shading Condition (PSC):

- MPPT: V = 38.6V, P = 115.0W
- PSO Reference Voltage (Vref): 38.4V
- The achieved Maximum Power Point (Pmpp): 114.5W

2. Second Partial Shading Condition (PSC):

- MPPT: V = 28.4V, P = 112.4W
- PSO Reference Voltage (Vref): 28.2V
- The achieved Maximum Power Point (Pmpp): 111.6W

3. Third Partial Shading Condition (PSC):

- MPPT: V = 28.5V, P = 71.5.0W
- PSO Reference Voltage (Vref): 28.4V
- The achieved Maximum Power Point (Pmpp): 70.9W

The results indicate that the PSO method accurately tracks the global maximum power point under varying partial shading conditions, with the MPPT values closely matching the reference voltages and power outputs. Although the PSO method provided precise Gmpp tracking, perturbations were observed in the voltage and power curves at the onset of each partial shading condition. These perturbations suggest that while the PSO method is effective in finding the global best results, the stability of the system, particularly at the transition points, could be improved. To enhance the stability and performance of the PV system, especially during the transition phases of partial shading conditions, we are going to use the Model-Free Control (MFC) in the next simulation.

3.5 Tracking MPP using PSO method and Model-Free control

In this study, we evaluat the performance of a photovoltaic (PV) system under partial shading conditions and varying irradianceas shown in the figures (fig(3.9), fig(3.10), fig(3.11), fig(3.12)) using the Particle Swarm Optimization (PSO) method for Global Maximum Power Point Tracking (MPPT) in conjunction with a model-free control (MFC) strategy. we are using the same conditions as the previous PSO simulation.The objective is to assess the accuracy of the PSO method in tracking the global maximum power point (Gmpp) and the stability of the system.

SIMULATION

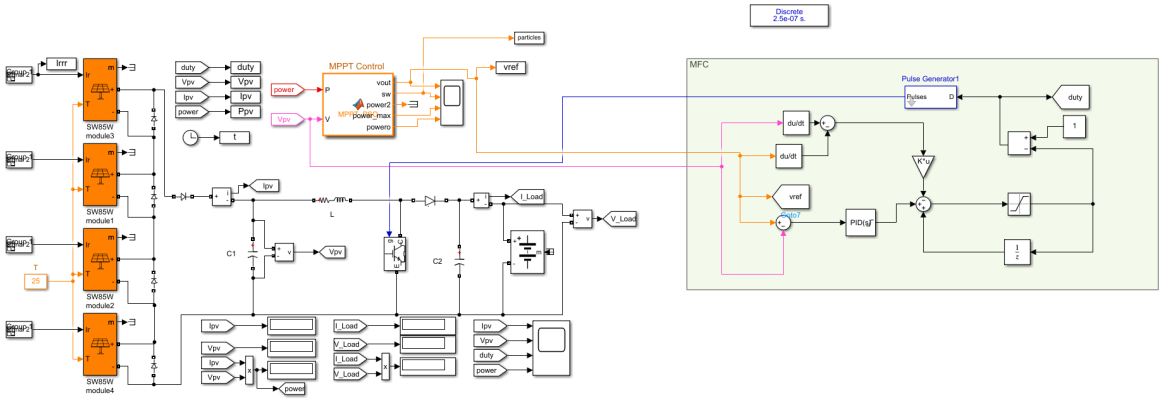

Figure 3.15: Simulation of PSO with MFC.

RESULT

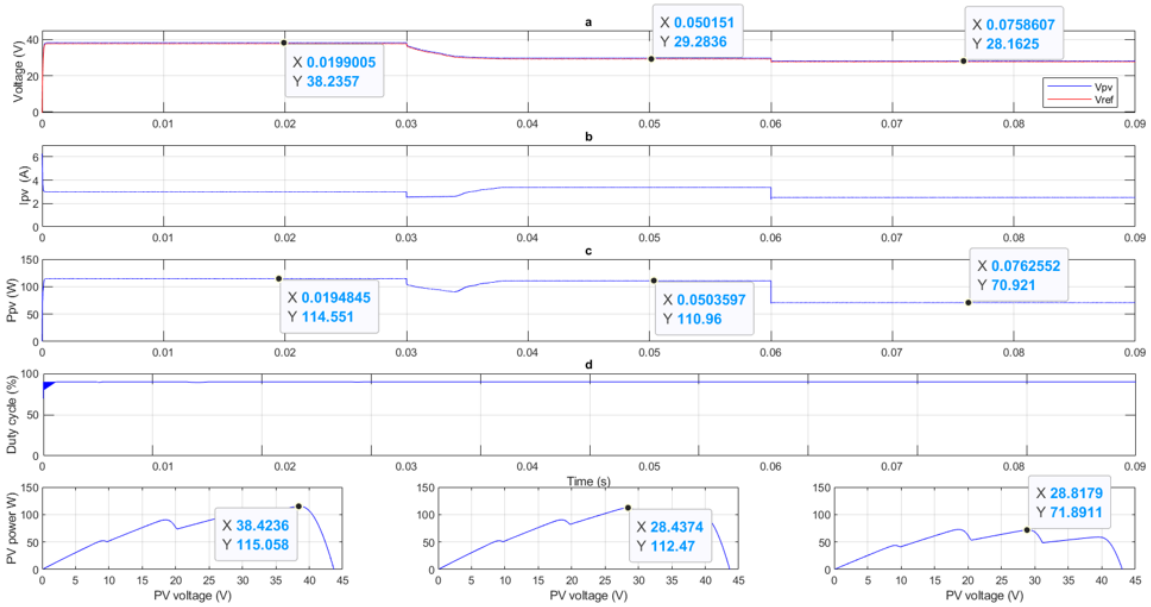

Figure 3.16: Results of PSO with MFC.

Simulation Results:

1. First Partial Shading Condition (PSC):

- MPPT: V = 38.4V, P = 115.0W
- PSO Reference Voltage (Vref): 38.2V
- Maximum Power Point (Pmpp): 114.5W

2. Second Partial Shading Condition (PSC):

- MPPT: V = 28.4V, P = 112.4W
- PSO Reference Voltage (Vref): 29.2V
- Maximum Power Point (Pmpp): 110.9W

3. Third Partial Shading Condition (PSC):

- MPPT: V = 28.8V, P = 71.8W
- PSO Reference Voltage (Vref): 28.1V
- Maximum Power Point (Pmpp): 70.9W

In the results of a photovoltaic (PV) system using a Particle Swarm Optimization (PSO) algorithm and Model-Free Control under varying irradiance conditions, demonstrate a highly effective performance in managing partial shading conditions (PSCs). Under the first PSC, occurring between $t = 0s$ and $t = 0.3s$, the system achieved a Maximum Power Point (MPPT) at 38.4V and 115.0W, with the PSO algorithm providing a reference voltage (V_{ref}) of 38.2V, resulting in a P_{mpp} of 114.5W. In the second PSC, occurring between $t = 0.3s$ and $t = 0.6s$, the MPPT was at 28.4V and 112.4W, with a V_{ref} of 29.2V and a P_{mpp} of 110.9W. For the third PSC, occurring between $t = 0.6s$ and $t = 0.9s$, the MPPT was at 28.8V and 71.8W, with a V_{ref} of 28.1V and a P_{mpp} of 70.9W. These results indicate that the PSO algorithm and Model-Free Control effectively track the maximum power points with minimal perturbations in voltage, power, and current curves, ensuring optimal performance under various shading scenarios.

3.6 Comparative Analysis

3.6.1 P&O with PI Regulation vs. P&O with MFC

The first simulation using the P&O algorithm and PI regulation showed promising results under varying irradiance levels. At 700 W/m², the simulated P_{mpp} was 59.8 W with V_{mpp} at 17.9 V, while the P&O and PI regulator achieved 58.6 W and V_{ref} at 17.7 V. At 500 W/m², the simulated P_{mpp} was 42.7 W with V_{mpp} at 17.9 V, and the achieved values were 42.5 W and V_{ref} at 17.8 V. These results indicate effective MPPT tracking, but the PI regulator introduced noticeable perturbations in the voltage, power, and current curves, highlighting a need for better regulation. Conversely, the second simulation using P&O with Model-Free Control (MFC) demonstrated superior performance. At 700 W/m², P&O and MFC achieved a P_{mpp} of 59.1 W with V_{ref} maintained at 17.9 V, and at 500 W/m², they attained a P_{mpp} of 42.1 W with V_{ref} again at 17.9 V. The results showed no perturbations in the voltage, power, and current curves, underscoring MFC's ability to enhance control stability and efficiency significantly over traditional PI regulation.

3.6.2 PSO with PID Regulation vs. PSO with MFC

The third simulation involving the PSO algorithm under partial shading conditions (PSCs) revealed the method's accuracy in tracking the global maximum power point. In the first

PSC, the MPPT values were $V = 38.6\,V$ and $P = 115.0\,W$, with the PSO Reference Voltage (V_{ref}) at 38.4 V, and the achieved P_{mpp} was 114.5 W. For the second PSC, the MPPT values were $V = 28.4\,V$ and $P = 112.4\,W$, with V_{ref} at 28.2 V, and the achieved P_{mpp} was 111.6 W. The third PSC showed MPPT values at $V = 28.5\,V$ and $P = 71.5\,W$, with V_{ref} at 28.4 V, and P_{mpp} at 70.9 W. Despite the accurate tracking, the system experienced perturbations in the voltage and power curves at the onset of each PSC, indicating a need for improved stability. The fourth simulation, integrating PSO with Model-Free Control (MFC), exhibited enhanced performance. Under the first PSC, the MPPT values were $V = 38.4\,V$ and $P = 115.0\,W$, with V_{ref} at 38.2 V, and P_{mpp} at 114.5 W. The second PSC showed MPPT values at $V = 28.4\,V$ and $P = 112.4\,W$, with V_{ref} at 29.2 V, and P_{mpp} at 110.9 W. The third PSC had MPPT values at $V = 28.8\,V$ and $P = 71.8\,W$, with V_{ref} at 28.1 V, and P_{mpp} at 70.9 W. These results demonstrated minimal perturbations and optimal performance, indicating the PSO and MFC method's superiority in handling PSCs.

3.6.3 PID Regulation vs. Model-Free Control (MFC)

Comparing PID regulation with Model-Free Control (MFC) across the simulations reveals MFC's clear advantage. In the first simulation, the PID regulator achieved acceptable MPPT performance, but introduced noticeable perturbations in the voltage, power, and current curves, affecting system stability. In the P&O with PI regulation simulation, perturbations were observed with V_{ref} at 17.7 V and 17.8 V for 700 W/m^2 and 500 W/m^2 respectively, while the corresponding power values were 58.6 W and 42.5 W. In contrast, MFC consistently maintained stable V_{ref} values and minimized perturbations, resulting in smoother voltage, power, and current curves. For instance, in the P&O with MFC simulation, V_{ref} remained at 17.9 V under both irradiance levels with power values of 59.1 W and 42.1 W. Similarly, in the PSO with MFC simulation, V_{ref} values were closely matched with MPPT values across all PSCs, with minimal perturbations. This superior performance indicates that MFC not only enhances control stability and efficiency but also ensures optimal performance under varying irradiance levels and partial shading conditions. The comparative results strongly suggest that MFC is an excellent choice for improving the stability and efficiency of PV systems over traditional PID regulation methods.

3.7 Conclusion

In conclusion, the four simulations conducted in this study provide valuable insights into the performance of different Maximum Power Point Tracking (MPPT) methods and control strategies for photovoltaic (PV) systems under varying conditions.

In the first simulation, the P&O algorithm combined with PI regulation showed that while the method is effective in tracking the MPPT, it introduced noticeable perturbations in the voltage, power, and current curves. This highlights the need for improved regulation to enhance stability and efficiency.

The second simulation, which integrated the P&O algorithm with Model-Free Control (MFC), demonstrated significant improvements. The results indicated that MFC effectively eliminated perturbations and maintained stable V_{ref} values, achieving smoother voltage, power, and current curves. This underscores the superior performance of MFC in enhancing control stability and efficiency over traditional PI regulation.

The third simulation involving the PSO algorithm under partial shading conditions (PSCs) showed accurate tracking of the global maximum power point. However, similar to the first simulation, perturbations were observed in the voltage and power curves at the onset of each PSC, indicating a need for better stability during transitions.

The last simulation, which combined the PSO algorithm with MFC, provided the best overall performance. It effectively tracked the maximum power points with minimal perturbations across all PSCs, demonstrating the superior capability of MFC in managing varying shading scenarios and enhancing system stability.

Finally, the comparative analysis across all simulations reveals that MFC consistently outperforms PID regulation by maintaining stable V_{ref} values and minimizing perturbations. These findings strongly suggest that adopting Model-Free Control in PV systems can significantly improve their stability, efficiency, and overall performance under varying irradiance levels and partial shading conditions.

General Conclusion

This thesis has explored and advanced the field of Maximum Power Point Tracking (MPPT) in photovoltaic (PV) systems through a comprehensive investigation into traditional and advanced control strategies. Chapter 1 provided a fundamental understanding of photovoltaic energy principles, the operation of solar cells, and the application of MPPT techniques, emphasizing the Perturb and Observe (P&O) algorithm under varying conditions, including Partial Shading Conditions (PSC). The implementation of P&O with a checking algorithm demonstrated its effectiveness in maximizing power output under dynamic environmental changes.

In Chapter 2, advanced control strategies were explored, focusing on Particle Swarm Optimization (PSO) and Model-Free Control (MFC). PSO was detailed as a robust optimization technique capable of efficiently locating the Global Maximum Power Point (GMPP) despite complex and dynamic system behaviors. The integration of PSO in MPPT for PV systems showcased its effectiveness in overcoming challenges posed by Partial Shading Conditions (PSC), enhancing the overall efficiency of MPPT algorithms.

Model-Free Control (MFC), discussed in depth in Chapter 2, introduced innovative approaches using intelligent PID controllers and the Ultra-Local Model to achieve adaptive MPPT without relying on explicit system models. The synergy between PSO and MFC demonstrated significant improvements in MPPT efficiency, leveraging PSO's global optimization capabilities with MFC's adaptive and model-free nature.

Chapter 3 extended these concepts by presenting a detailed simulation study of a PV system integrating GPV with MPPT control, validating the effectiveness of PSO and MFC strategies in real-world scenarios. The simulation results underscored the superiority of integrated PSO and MFC approaches in maximizing power extraction under diverse operating conditions, thereby enhancing the reliability and performance of PV systems.

Future research in photovoltaic (PV) systems should prioritize enhancing Model-Free

Control (MFC) algorithms for improved adaptability, developing dynamic adjustment mechanisms to optimize energy harvesting efficiency, exploring hybrid control approaches for enhanced system performance, advancing sensing and feedback systems for accurate real-time data, and conducting cross-validation studies with emerging MPPT methods to validate effectiveness across different PV system configurations. These efforts aim to enhance the reliability, efficiency, and adaptability of PV systems under varying operational conditions.

In conclusion, this thesis has contributed to advancing the state-of-the-art in MPPT for PV systems by providing a comprehensive analysis of traditional and advanced control strategies. The integration of Particle Swarm Optimization and Model-Free Control has shown promising results in overcoming the challenges of dynamic environmental conditions and partial shading, offering new insights and methodologies for optimizing the efficiency and reliability of photovoltaic energy systems.

Bibliography

[1] U.S. Energy Information Administration. Equivalent circuit model of a solar cell.

[2] Bourahla Ahmed and Dabouz Mustapha. Etude et applications d'une commande par la méthode model free control application sur la commande mppt d'un gpv. Mémoire de master, Université Amar Telidji - Laghouat, Laghouat, Algeria, 2018. Promotion: 2017-2018.

[3] Rozana Alik, Awang Jusoh, and Tole Sutikno. A study of shading effect on photovoltaic modules with proposed p&o checking algorithm. International Journal of Electrical & Computer Engineering (2088-8708), 7(1), 2017.

[4] Muhannad Alshareef, Zhengyu Lin, Mingyao Ma, and Wenping Cao. Accelerated particle swarm optimization for photovoltaic maximum power point tracking under partial shading conditions. Energies, 12:623, 02 2019.

[5] Djamel Bendahou and El-Abbes Bourouis. Commande mppt pour les systèmes photovoltaïques en utilisant l'optimisation par essaim de particules, 2013. Année Universitaire 2012-2013.

[6] Christian Blum and Daniel Merkle. Swarm Intelligence: Introduction and Applications. Natural Computing Series. Springer-Verlag, Berlin Heidelberg, 2008.

[7] Youssef Chaibi, A. Allouhi, M. Salhi, et al. Annual performance analysis of different maximum power point tracking techniques used in photovoltaic systems. Protection and Control of Modern Power Systems, 4:15, 2019.

[8] U.S. Energy Information Administration (EIA). Photovoltaics and electricity.

[9] I.C. Ezeonu, J.P. Iloh, M.O. Ogamba, and A.O. Elukpo. Performance comparism between perturb and observe -particle swarm optimization (po- pso) and perturb and observe algorithm for maximum power point tracking in photovoltaic systems. 4:163–173, 03 2021.

[10] Muhammad Yaqoob Javed, Adeel Feroz Mirza, Ali Hasan, Syed Tahir Hussain Rizvi, Qiang Ling, Muhammad Majid Gulzar, Muhammad Umair Safder, and Majad Mansoor. A comprehensive review on a pv based system to harvest maximum power. Electronics, 8(12):1480, 2019.

[11] Cédric Join, Frédéric Chaxel, and Michel Fliess. programmable devices.

[12] Sena Kaynarkaya and Gulen Cagdas. Evaluation of metro lines with swarm intelligence approach. Journal of Information Technology in Construction, 27:802–826, 08 2022.

[13] AMEUR Khaled. Contribution to the study of a standalone photovoltaic system with a new tracking control of the global mpp. University Amar Telidji of Laghouat," April, 2018.

[14] Sanko Power. Pv panel model. https://www.sankopower.com/img/n1.jpg, 2021. Accessed: 2021.

[15] Ahlam Shakoor and Hersh Taha. Modelling and simulation of perturb and observe mppt algorithm based on the pi controller for photovoltaic system. Kurdistan Journal of Applied Research, pages 71–83, 11 2022.

[16] Kenneth Teo, Pei Lim, Bih Lii Chua, Hui Hwang Goh, and Min Keng Tan. Maximum power point tracking of partially shaded photovoltaic arrays using particle swarm optimization. pages 247–252, 12 2014.

[17] Kenneth Tze Kin Teo, Pei Yi Lim, Bih Lii Chua, Hui Hwang Goh, and Min Keng Tan. Maximum power point tracking of partially shaded photovoltaic arrays using particle swarm optimization. In 2014 4th International Conference on Artificial Intelligence with Applications in Engineering and Technology, pages 247–252. IEEE, 2014.

[18] TheGreenAge. Types of solar panel, 2014. Accessed: 2024-06-03.